Serum Citrulline and Ornithine: Potential Markers of Coeliac Disease Activity

Ladislav Douda[1], Radomír Hyšpler[2], Martin Mžik[2], Doris Vokurková[3], Marcela Drahošová[3], Vít Řeháček[4], Eva Čermáková[5], Tomáš Douda[1], Jiří Cyrany[1], Tomáš Fejfar[1], Václav Jirkovský[1], Marcela Kopáčová[1], Blanka Kupková[1], Tomáš Vašátko[1], Ilja Tachecí[1,*], Jan Bureš[6]

ABSTRACT

Introduction: To date, there is not generally accepted and universal indicator of activity, and functional integrity of the small intestine in patients with coeliac disease. The aim of our study was to investigate whether serum concentrations of the non-essential amino acids citrulline and ornithine might have this function.

Methods: We examined serum citrulline and ornithine concentrations in a subgroup of patients with proven coeliac disease and healthy controls (blood donors).

Results: A total of 94 patients with coeliac disease (29 men, mean age 53 ± 18 years; 65 women, mean age 44 ± 14 years) and 35 healthy controls (blood donors) in whom coeliac disease was serologically excluded (10 men, mean age 51 ± 14 years; 25 women, mean age 46 ± 12 years) were included in the study. Significantly lower concentrations of serum ornithine were found in patients with coeliac disease (mean 65 ± 3 µmol/L; median 63 µmol/L, IQR 34 µmol/L, $p < 0.001$). No statistically nor clinically significant differences were found in the citrulline concentrations between the study and control group.

Conclusions: Serum ornithine (but not citrulline) may be useful for assessing the functional status of the small intestine in uncomplicated coeliac disease. Further studies involving more detailed analysis of dietary and metabolic changes in patients will be needed to reach definitive conclusions.

KEYWORDS

coeliac disease; citrulline; ornithine

AUTHOR AFFILIATIONS

[1] 2nd Department of Internal Medicine – Gastroenterology, Charles University, Faculty of Medicine in Hradec Králové and University Hospital Hradec Králové, Czech Republic
[2] Institute of Clinical Biochemistry and Diagnostics, Charles University, Faculty of Medicine in Hradec Králové and University Hospital Hradec Králové, Czech Republic
[3] Department of Clinical Immunology and Allergology, Charles University, Faculty of Medicine in Hradec Králové and University Hospital Hradec Králové, Czech Republic
[4] Transfusion Department, University Hospital Hradec Králové, Czech Republic
[5] Department of Medical Biophysic, Charles University, Faculty of Medicine in Hradec Králové, Czech Republic
[6] Biomedical Research Centre, University Hospital Hradec Králové, Hradec Králové, Czech Republic
* Correspondent author: 2nd Department of Internal Medicine – Gastroenterology, Faculty of Medicine in Hradec Králové, Charles University and University Hospital Hradec Králové, Sokolská 581, 500 05 Hradec Králové, Czech Republic; e-mail: ilja.tacheci@fnhk.cz

Received: 14 October 2022
Accepted: 15 December 2022
Published online: 2 February 2023

Acta Medica (Hradec Králové) 2022; 65(3): 75–82
https://doi.org/10.14712/18059694.2022.22

INTRODUCTION

Coeliac disease is a chronic, immune-mediated, and gluten-associated disease in genetically susceptible individuals (1, 2). The term "gluten-associated" more precisely describes its multisystemic nature. Other diseases may be associated with gluten intake too (3), which in fact, among the other things, makes the research and results interpretation difficult (4). Coeliac disease is a relatively common disorder with an average prevalence in Europe of 1% and in the Czech Republic up to 1 : 200 (2, 4, 5). On the contrary, mainly due to the frequent oligosymptomatic or asymptomatic course, coeliac disease is poorly considered in diagnostic algorithms and it is estimated that it is diagnosed early and correctly only in 10–15% of cases (6, 7).

The diagnostic approach in routine clinical practice is based on the determination of serum levels of antibodies against tissue transglutaminase (IgA class) and histological examination of biopsy samples of duodenal mucosa (1, 2, 4, 8). Small intestinal involvement plays a dominant role in the diagnosis and clinical manifestation of disease (1, 9). The characteristic histological picture of coeliac disease is an increased number of intraepithelial lymphocytes, crypt hyperplasia and especially atrophy of the small intestinal villi (10, 11). Villous atrophy is not specific to coeliac disease and may accompany several other enteropathies (1, 8). Although usually uncomplicated forms of coeliac disease do not primarily lead to significant intestinal dysfunction (12, 13), the disease can lead to malabsorption syndrome, including iron, trace element and vitamin deficiencies, and malnutrition. When intestinal function is reduced below the minimum necessary for absorption of macronutrients and/or water and electrolytes, so that intravenous supplementation is required to maintain health and/or growth, we speak of intestinal failure (12, 14–18). Patients with coeliac disease have an increased risk of developing serious complications – refractory coeliac disease, ulcerative jejunoileitis and/or small intestinal malignancies. In the presence of at least one of the above-mentioned conditions we speak about "complicated" coeliac disease and in their absence of "uncomplicated" coeliac disease (4, 19, 20).

A reliable indicator for assessing small bowel function is not yet available in patients with uncomplicated coeliac disease (4). One possible candidate marker is citrulline. It is a non-essential, non-protein (non-biogenic) amino acid whose biological potential was thought to be low for many years and has been identified in the human body only as an intermediate in the urea cycle and amino acid metabolism. Since 2000, some data have appeared in the literature on the role of circulating citrulline as a possible marker of functional integrity of the small intestine and villous atrophy in various enteropathies, including coeliac disease (21, 22). The role of citrulline in the body has been found to be complex, including its effect on the cardiovascular system (23), its antioxidant and immunomodulatory effects (24, 25), and especially its role in maintaining nitrogen homeostasis (26, 27). Interesting in this context is also the question of the possibility of using some of the precursors of citrulline, which are part of its synthesis in the enterocyte, for example ornithine or arginine and its correlation with citrulline levels. Clear data in this area are still lacking in the literature.

MATERIAL AND METHODS

The project was designed as a case-control study comparing a group of patients with previously diagnosed coeliac disease and healthy volunteers (blood donors). Inclusion criteria were a diagnosis of coeliac disease based on a combination of positive serology (always including anti-transglutaminase IgA) and histology. All patients underwent upper endoscopy with duodenal biopsy sampling at the time of initial diagnosis.

In control group of healthy donors, the coeliac disease was serologically excluded by means of negative results of multiple serum antibodies (anti-tissue transglutaminase IgA and IgG, anti-endomysial IgA and IgG, DGP (anti-deamidated gliadin peptide) IgA and IgG and anti-reticulin IgA and IgG).

A venous blood samples from patients and healthy controls (irrespective of fasting) were collected on a separation gel followed by centrifugation (2000 g gravity, 20 degrees Celsius) and freezing (–80 degrees Celsius) until final analysis. Then, an ultrahigh-performance liquid chromatography (Ultimate 3000 RS pump Dionex, Thermo Scientific, San Jose, CA, USA) coupled with high-resolution mass spectrometer with orbitrap analyser (Q-Exactive Focus, Thermo Scientific, San Jose, CA, USA) was used in quantitative analyses of citrulline and ornithine in serum. Sample preparation was based on previously published method using pentafluorobenzoyl chloride as derivatization reagent (28). Isotopically labelled citruline-d_4 and ornithine-d_6 were used as internal standards. Chromatographic separation with mass spectrometry analysis was developed and optimized, followed by full method validation according to the Guideline on Bioanalytical Method Validation (29). All evaluated parameters met the required criteria proving the method to be precise and accurate. Certified lyophilised calibration and control materials (RECIPE Chemicals + Instruments GmbH, Munich, Germany) were used during study.

The obtained data were processed using methods of descriptive statistics. Data by normal distribution of values were further analysed by parametric two-sample t-test and the data with non-normal distribution were tested by non-parametric Mann-Whitney and Kolmogorov-Smirnov test. For qualitative parameters the Fisher's exact test was used. For correlation analysis the Spearman's rank correlation coefficient was used. For the above-mentioned statistical analysis was used NCSS 2021 Statistical Software (NCSS, LLC, Kaysville, Utah, USA, 2021: ncss.com/software/ncss). The study was approved by the Joint University Ethics Committee (Reference number: 202 107 PO6). All procedures were in accordance with the ethical standards of the institutional research committee and with the 1964 Helsinki declaration and its latter amendments (30). All patients signed written consent. For all data obtained, all personal identification information were deleted in compliance with the laws for the protection of confidentiality of the Czech Republic.

RESULTS

Two subgroups entered the study: the study group of 94 patients with coeliac disease and the control group of 35 healthy blood donors. The age and sex structure of the study group was 29 men (31%), mean age 53 ± 18 years (median: 47 years, interquartile range: 31 years) and 65 women (69%), mean age 44 ± 14 years (median: 41 years, interquartile range: 20 years) – details in Table 1. The age and gender structure of the controle group consisted of 10 men (29%), mean age 51 ± 14 years (median 47 years, interquartile range 19 years) and 25 women (71%), mean age 46 ± 12 years (median 45 years, interquartile range 18 years) – details in Table 1.

The mean disease duration (in the group of coeliac disease patients) was 160 ± 144 months, median: 118 months (interquartile range: 181 months). The most common histological finding in coeliac disease patients was type 3a according to the Marsh-Oberhuber classification. None of the patients underwent small bowel resection and/or splenectomy. Some autoimmune-associated diseases occurred in the group of patients: rheumatoid arthritis (1 case), autoimmune thyreopathy (19 cases), atopic dermatitis (4 cases), vitiligo (3 cases), autoimmune hepatitis (1 case), IgM nefropathy (1 case), type 1 diabetes mellitus (5 cases), asthma bronchiale (12 cases), polyserositis (1 case), antiphospholipid syndrome (1 case), systemic sclerosis (2 cases), autoimmune gastritis (1 case), spondylarthritis (1 case), psoriasis (2 cases), eosinophilic oesophagitis (1 case), hereditary angioedema (1 case). There was no patient with associated Sjögren syndrome. IgA deficiency was found in four patients and in no healthy control. HLA genotyping was not performed in either patients or healthy controls. The patient did not include a person with current acute (or acute on chronic) kidney injury that could affect serum citrulline and/or ornithine concentrations.

In a statistical survey of patients with coeliac disease and group of healthy controls (blood donors), their quantitative and qualitative features were monitored and compared. In the monitoring of quantitative traits, emphasis was placed on serum concentrations of citrulline and ornithine as possible indicators of small intestinal function and total enterocyte mass.

Serum ornithine concentrations showed a statistically significant differences between the group of patients with coeliac disease and the group of healthy controls ($p < 0.001$). The statistically significant differences were identified in serum transglutaminase IgA concentration ($p = 0.024$) too (other monitored clinical and laboratory

Tab. 1 Basic quantitative features in patients with coeliac disease and healthy controls (blood donors). SD – standard deviation, NS – not significant, S – significant, µmol – micromol, U – unit, L – litre, IQR – interquartile range, n = number of subjects, BMI = body mass index, BSA = body surface area, MCV = mean corpuscular volume.

Parameter	Controls (n = number of subjects; mean ± SD; median; IQR)	Coeliac disease (n = number of subjects; mean ± SD; median; IQR)	Statistical significance
Age (years)	n = 35 47 ± 13 47; 18	n = 94 46 ± 16 43; 21	NS (p = 0.372)
Weight (kilograms)	n = 35 82 ± 22 75; 23	n = 94 70 ± 16 68; 21	NS (p = 0.062)
BMI (kg/m$^{2)}$	n = 35 27 ± 4 27; 6	n = 94 25 ± 5 24; 6	S (p = 0.006)
BSA (m$^{2)}$	n = 35 1,8 ± 0,2 1,8; 0,3	n = 94 1,7 ± 0,2 1,7; 0,3	S (p = 0.011)
Haemoglobin (g/L)	n = 35 142 ± 10 141; 13	n = 94 137 ± 13 138; 15	NS (p = 0.072)
Leukocytes (10^{9}/L)	n = 35 7 ± 2 6; 2	n = 94 7 ± 2 7; 3	NS (p = 0.814)
MCV (fL)	n = 35 90 ± 4 91; 5	n = 94 87 ± 5 87; 5	S (p = 0.002)
Transglutaminase IgA (U/mL)	n = 35 2 ± 2 2; 1	n = 88 12 ± 42 3; 4	S (p = 0.024)
Citrulline (µmol/L)	n = 35 30 ± 10 29; 10	n = 94 27 ± 10 27; 15	NS (p = 0.136)
Ornithine (µmol/L)	n = 35 97 ± 26 97; 42	n = 94 65 ± 3 63; 34	S (p < 0.001)

markers in Table 1). Due to the mostly rejected normality, the median and interquartile ranges (75th percentile minus 25th percentile) were used to express the degree of variability in addition to the arithmetic mean and standard deviation values. Correlation analysis using the nonparametric Spearman's rank correlation coefficient proved statistically significant stronger correlation between plasma citrulline and ornithine concentrations in the group of patients with coeliac disease (Spearman's coefficient = 0.723) versus the group of healthy controls where the correlation was weak (0.723 vs. 0.313; Table 2, Figure 1) (31). We did not find a strong correlation between disease duration and serum citrulline and / or ornithine concentrations.

For other quantitative features no strong correlation rate was found in the group of patients with coeliac disease and healthy controls (Table 3).

The main qualitative characteristic monitored was smoking. There was a total of 13 smokers (14%) in the group of patients (5 men (39%), 8 women (61%)), and 5 smokers (14%) in the control group (2 men (40%), 3 women (60%)). We did not find any significant differences in the serum concentrations of citrulline and ornithine in smokers and non-smokers in the two groups studied (Table 4 and 5).

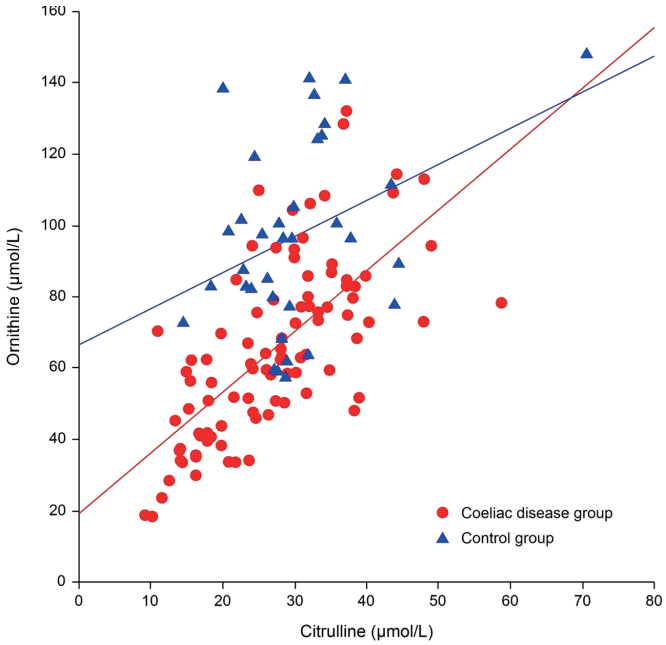

Fig. 1 Correlation of serum citrulline and ornithine concentrations in the group of patients with coeliac disease (Spearman's coefficient = 0.723) and healthy controls (Spearman's coefficient = 0.313).

Tab. 2 Correlation between other quantitative traits and serum concentrations of citrulline and ornithine in the group of coeliac patients (expressed by Spearman's coefficient). M – males, F – females, SD – standard deviation, µmol – micromol, U – unit, L – litre, IQR – interquartile range, n = number of subjects.

Parameter	**Citrulline – total** (M / F)	**Correlation strength**	**Ornithine – total** (M / F)	**Correlation strength**
Age (years)	0.215 (0.081 / 0.261)	weak (very weak / weak)	0.303 (-0.002 / 0.431)	weak (very weak /medium)
Weight (kilograms)	-0.066 (-0.079 / -0.105)	very weak (very weak / very weak)	0.093 (0.007 / 0.082)	very weak (very weak/ very weak)
BMI (kg/m^2)	0.027 (0.126 / -0.001)	very weak (very weak / very weak)	0.138 (0.149 / 0.124)	very weak (very weak/ very weak)
BSA (m^2)	-0.132 (-0.185 / -0.169)	very weak (very weak / very weak)	0.072 (-0.062 / 0.055)	very weak (very weak / very weak)
Haemoglobin (g/L)	0.111	very weak	0.042	very weak
Leukocytes (10^9/L)	-0.0445	very weak	-0.074	very weak
MCV (fL)	-0.064	very weak	0.028	very weak
Transglutaminase IgA (U/mL)	-0.206	weak	-0.065	very weak
Disease duration (months)	-0.0305	very weak	0.0047	very weak

Tab. 3 Correlation between other quantitative traits and serum concentrations of citrulline and ornithine in the group of healthy controls (expressed by Spearman's coefficient). M – males, F – females, SD – standard deviation, µmol – micromol, U – unit, L – litre, IQR – interquartile range, n = number of subjects.

Parameter	**Citrulline –total** (M / F)	**Correlation strenght**	**Ornithine – total** (M / F)	**Correlation strenght**
Age (years)	0.375 (0.610 / 0.204)	weak (strong / weak)	0.132 (-0.553 / 0.345)	very weak (medium / weak)
Weight (kilograms)	0.101 (-0.330 / 0.073)	very weak (weak / very weak)	0.119 (-0.128 / 0.144)	very weak (very weak / very weak)
BMI (kg/m^2)	0.027 (-0.430 / 0.002)	very weak (medium / very weak)	0.232 (0.139 / 0.233)	weak (very weak / weak)
BSA (m^2)	0.128 (-0.321 / 0.070)	very weak (weak / very weak)	0.221 (-0.079 / 0.284)	weak (very weak / weak)
Haemoglobin (g/L)	0.105	very weak	-0.125	very weak
Leukocytes (10^9/L)	-0.510	medium	-0.245	weak
MCV (fL)	0.092	very weak	-0.086	very weak
Transglutaminase IgA (U/mL)	-0.175	very weak	-0.027	very weak

Tab. 4 Serum concentrations of citrulline and ornithine in the group of patients with coeliac disease in relation to smoking. SD – standard daviation, NS – not significant, S – significant, µmol – micromol, L – litre, IQR – interquartile range, n = number of subjects.

Parameter	Smoking – YES (n = number of subjects; mean ± SD; median; IQR)	Smoking – NO (n = number of subjects; mean ± SD; median; IQR)	Statistical significance
Citrulline (µmol/L)	n = 13 26 ± 10 22; 15	n = 81 27 ± 10 27; 15	NS (p = 0.579)
Ornithine (µmol/L)	n = 13 69 ± 29 62; 41	n = 81 65 ± 24 63; 33	NS (p = 0.550)

Tab. 5 Serum concentrations of citrulline and ornithine in a group of healthy controls in relation to smoking. SD – standard daviation, NS – not significant, S – significant, µmol – micromole, L – litre, IQR – interquartile range, n = number of subjects.

Parameter	Smoking – YES (n = number of subjects; mean ± SD; median; IQR)	Smoking – NO (n = number of subjects; mean ± SD; median; IQR)	Statistical significance
Citrulline (µmol/L)	n = 5 28 ± 4 28; 7	n = 30 31 ± 10 29; 11	NS (p = 0.588)
Ornithine (µmol/L)	n = 5 97 ± 29 98; 50	n = 30 97 ± 26 97; 43	NS (p = 0.948)

DISCUSSION

The aim of this study was to investigate the significance of serum amino acids citrulline and ornithine as potential non-invasive markers of small intestinal damage in patients with coeliac disease. The main finding of our study is statistically significantly lower serum ornithine concentrations in patients with uncomplicated coeliac disease compared to healthy controls. On the other hand, no statistically significant difference in serum citrulline concentrations was found.

The diagnosis of coeliac disease is currently well defined, based on a combination of positive serological markers (positive antibodies to tissue transglutaminase IgA, TTG IgA) and a typical histological picture in the small intestinal mucosa (1, 2, 4, 8, 10, 11). On the other hand, there is still no reliable indicator of celiac disease activity to monitor patients (4). In real clinical practice, the "gold" standard of disease monitoring remains the determination of specific autoantibodies and invasive histological examination of biopsy samples from duodenal mucosa (1, 2, 4, 8) – however, this approach has several problematic moments and, in some cases, fails. The serological activity of coeliac disease-specific autoantibodies may be difficult to interpret in immunocompromised patients (e.g. immunodeficiency conditions including IgA deficiency, immunomodulatory treatment for another diagnosis). Other areas reducing the usefulness of serological markers in monitoring coeliac disease activity are immune dysregulation, as evidenced by the frequently associated functional hyposplenism and selective memory B-lymphocyte deficiency (32) and the so-called seronegative coeliac disease (4) with the inability of TTG IgA to leave the mucosa into the bloodstream (33). Moreover, the dynamics of the serological response can be misleading. Although a reduction in serum TTG IgA concentrations indicates the effect of a gluten-free diet and is a marker of reduced disease activity (34), an antibody response (and thus serologic detection of TTG IgA) may not be present when less gluten is re-consumed.

In these cases, TTG IgA sensitivity decreases and does not reflect the severity of histological changes in the small intestinal mucosa (8). Even changes in histological findings in the small intestine may not be a reliable indicator of the course of the disease. Histological changes mimicking coeliac disease occur e.g. with commonly available and used drugs (NSAIDs, PPIs). Moreover, histological monitoring is a relatively invasive approach. In view of this, intensive efforts are being made to find new non-invasive markers of the functional status of the small intestine.

The first findings of the biological nature and function of citrulline and its relationship to the small intestine were provided by Windmüller et al. (35). Since 2000, Crenn et al. presents citrulline as a possible laboratory indicator of intestinal failure and diseases associated with villous atrophy (21, 22). There is a strong correlation between serum citrulline levels and the severity of small bowel failure (which is well and precisely defined), but the diagnosis of intestinal failure remains relatively rare (12, 17) and uncomplicated coeliac disease is not a common cause of intestinal failure (13, 15). Although citrulline has been the subject of other published studies (22–40) describing its relationship to intestinal diseases (plasma concentrations reliably reflect the total functional mass of enterocytes) (22, 36–41), its determination is not well defined in routine clinical practice. An important precursor of citrulline in enterocytes is ornithine, whose role in relation to intestinal diseases is unclear (42, 43). Citrulline is found in the body in two forms (free citrulline and citrullinated proteins) (44), and the main site of its synthesis from dietary arginine, glutamine and proline (via ornithine as a direct precursor) is the small intestine (mainly the abo-

ral ileum) (35, 42, 44). In this context, it should be noted that enterocytes are equipped with transport systems that also allow efficient uptake of luminal citrulline (45, 46). Citrulline is released from enterocytes into the portal circulation (not taken up by the liver) and continues to the cells of the proximal renal tubule, where undergo its final conversion to arginine (35, 42, 47, 48). Arginine is then available through the systemic circulation to the whole body for proteosynthesis. This metabolic pathway (arginine / glutamine – ornithine – citrulline) plays an important role in maintaining the body's nitrogen homeostasis (42). Citrullin is involved in the post-translational modification of some proteins (citrullination) (48) and several diseases (e.g. rheumatoid arthritis, psoriasis and multiple sclerosis) are associated with the presence of citrullinated proteins or antibodies against them (49–54). Ornithine is involved in complex metabolic processes (regulation of growth hormone production, lipolysis and immunomodulation) and the urease cycle (37, 55).

Literature data suggest the utility of plasma citrulline levels to monitor disease severity in patients with extensive and/or destructive involvement of the small intestinal mucosa (including complicated forms of coeliac disease such as refractory coeliac disease, ulcerative jejunoileitis and T-cell lymphoma-associated enteropathy), which can lead to small bowel failure and/or malabsorption syndrome (12, 13), rather than for patients with uncomplicated forms of coeliac disease (22, 56). All patients included in our study had previously diagnosed coeliac disease and were treated with a gluten-free diet with significant clinical effect (no patient had clinically active disease). None of the patients had laboratory evidence of intestinal failure or malabsorption syndrome. Although we found some statistically significant differences in body mass index (BMI, $p = 0.006$), body surface area (BSA, $p = 0.011$) and mean corpuscular volume (MCV, $p = 0.002$) between patients with coeliac disease and healthy controls, these findings could not be considered clinically significant (given the relatively low values) – Table 1. Considering this, and completely in accordance with the literature data, no statistically significant difference in serum citrulline levels was found between coeliac patients and healthy controls in our study.

Although the statistically significantly lower plasma concentrations of ornithine found in our study in patients with uncomplicated coeliac disease ($p < 0.001$) compared to healthy controls might suggest its greater sensitivity compared to citrulline as a marker of small intestinal mucosal damage, other explanations for this finding have been offered. One explanation may be changes in serum levels of various amino acids caused by differences between individuals on gluten-free and regular diets (blood donors in our cohort). Citrulline is a specific product of enterocytes and is not present in the diet (with the exception of melons) (57) and is not released by other cells (both study groups, i.e., coeliac patients and a control group of healthy blood donors, were not burdened by a diet containing melons). In contrast, ornithine is common in the diet and its daily intake is a few grams. However, an important fact is its association with another amino acid, arginine, which is a substrate for the formation of ornithine. It is the reduced dietary intake of arginine in patients on a gluten-free diet that may theoretically contribute to lower serum ornithine levels (58). From this perspective, a possible effect of fasting on serum ornithine levels cannot be excluded. However, the levels of both amino acids (citrulline and ornithine) were examined in our study in non-fasting patients and/or healthy controls. In addition, gluten itself stimulates the activity of arginase (the enzyme required to convert arginine to ornithine), and therefore a gluten-free diet may also lead by this mechanism to lower production and reduced serum ornithine concentrations (59).

It is a question (or rather speculation) whether the above statements can explain the surprisingly statistically significant correlation between plasma concentrations of citrulline and ornithine in the group of patients with coeliac disease compared to the group of healthy controls, where the correlation was weak (Table 2, Figure 1). In view of this, it will be necessary to verify our data by a more detailed analysis of the dietary amino acid content and metabolic changes in their production.

Our study has some important limitations. The main one is the lack of longitudinal monitoring of the observed changes in serum amino acid levels over time and the lack of correlation with invasive tests (histological changes in the small intestinal mucosa) and more detailed nutritional parameters analysis (including serum iron levels, ferritin, etc.). A minor limitation is the absence of HLA genotyping in the group of healthy controls to definitively exclude seronegative coeliac disease, although its probability in this group is low.

CONCLUSIONS

There is still no universal and generally accepted indicator of coeliac disease activity, especially in patients with uncomplicated coeliac disease. The non-essential amino acids citrulline and ornithine and their determination in serum seem to be suitable candidates. Serum ornithine might be more sensitive for assessing disease activity in patients with coeliac disease without intestinal failure and/or malassimilation syndrome. Further studies will be needed to confirm our results, especially focusing on the effects of diet and metabolic changes on the serum levels of specific amino acids.

ACKNOWLEDGEMENTS

This work was supported by the Cooperatio Program, research area INDI.

REFERENCES

1. Al-Toma A, Volta U, Auricchio R, et al. European Society for the Study of Coeliac Disease (ESsCD) guideline for coeliac disease and other gluten-related disorders. United European Gastroenterol J 2019; 7(5): 583–613.
2. Bai J, Ciacci C, Corazza G, et al. World Gastroenterology Organisation Global Guidelines: Celiac disease. Milwaukee: World Gastroenterology Organisation, 2016, http://wwwworldgastroenterologyorg /guidelines/global- guidelines/celiac-disease/celiac-disease-english (accessed 2017-08-08).

3. Helms S. Celiac disease and gluten-associated diseases. Altern Med Rev 2005; 10(3): 172–92.
4. Bureš J. Coeliac disease and other gluten-associated diseases. 2017. (in Czech)
5. Bulletin of the Ministry of Health of the Czech Republic; 28.2.2011; part 3. Targeted screening for coeliac disease (methodical guideline). Prague: Ministry of Health of the Czech Republic, 2011. (in Czech)
6. Frič P. Coeliac sprue (p. 219–38). In: Bureš J et al. Gastroenterology 2006. Collectio novissima. Prague: Triton, 2006. (in Czech)
7. Frič P, Zavoral M, Dvořáková T. Diseases caused by gluten. Vnitř Lék 2013; 59: 376–82. (in Czech)
8. Lebwohl B, Green PHR. New Developments in Celiac Disease. Gastroenterol Clin North Am 2019; 48(1): xv–xvi.
9. Bureš J. Endoscopic features of coeliac disease. Folia Gastroenterol Hepatol, 2005.
10. Marsh MN. Gluten, major histocompatibility complex, and small intestine. A molecular and immunobiologic approach to the spectrum of gluten sensitivity ('celiac sprue'). Gastroenterology 1992; 102: 330–5.
11. Oberhuber G, Granditsch G, Vogelsang H. The histopathology of celiac disease: time for a standardized report scheme for pathologists. Eur J Gastroenterol Hepatol 1999; 11: 1185–94.
12. Pironi L, Konrad D, Brandt C, et al. Clinical classification of adult patients with chronic intestinal failure due to benign disease: An international multicenter cross-sectional survey. Clin Nutr 2018; 37(2): 728–38.
13. Ng KYB, Mehta R, Mohamed S, Mohamed Z, Arnold J. Severe Refractory Coeliac Disease with Response Only to Parenteral Nutrition. Case Rep Gastroenterol 2014; 8(3): 297–303.
14. O'Keefe SJ, Buchman AL, Fishbein TM, Jeejeebhoy KN, Jeppesen PB, Shaffer J. Short bowel syndrome and intestinal failure: consensus definitions and overview. Clin Gastroenterol Hepatol 2006; 4(1): 6–10.
15. Pironi L, Arends J, Bozzetti F, et al. ESPEN guidelines on chronic intestinal failure in adults. Clin Nutr 2016; 35(2): 247–307.
16. Bharadwaj S, Tandon P, Meka K, et al. Intestinal Failure: Adaptation, Rehabilitation, and Transplantation. J Clin Gastroenterol 2016; 50(5): 366–72.
17. Kappus M, Diamond S, Hurt RT, Martindale R. Intestinal Failure: New Definition and Clinical Implications. Curr Gastroenterol Rep 2016; 18(9): 48.
18. Klek S, Forbes A, Gabe S, et al. Management of acute intestinal failure: A position paper from the European Society for Clinical Nutrition and Metabolism (ESPEN) Special Interest Group. Clin Nutr 2016; 35(6): 1209–18.
19. Penny HA, Schiepatti A, Sanders DS. Chapter 5 – Nonresponsive and complicated coeliac disease. In: Schieptti A, Sanders D, editors. Coeliac Disease and Gluten-Related Disorders: Academic Press; 2022, p. 87–100.
20. Ludvigsson JF, Leffler DA, Bai JC, et al. The Oslo definitions for coeliac disease and related terms. Gut 2013; 62(1): 43–52.
21. Crenn P, Coudray-Lucas C, Thuillier F, Cynober L, Messing B. Postabsorptive plasma citrulline concentration is a marker of absorptive enterocyte mass and intestinal failure in humans. Gastroenterology 2000; 119(6): 1496–505.
22. Crenn P, Vahedi K, Lavergne-Slove A, Cynober L, Matuchansky C, Messing B. Plasma citrulline: A marker of enterocyte mass in villous atrophy-associated small bowel disease. Gastroenterology 2003; 124(5): 1210–9.
23. Romero MJ, Platt DH, Caldwell RB, Caldwell RW. Therapeutic use of citrulline in cardiovascular disease. Cardiovasc Drug Rev 2006 Fall-Winter; 24(3–4): 275–90.
24. Akashi K, Miyake C, Yokota A. Citrulline, a novel compatible solute in drought-tolerant wild watermelon leaves, is an efficient hydroxyl radical scavenger. FEBS Lett 2001 Nov 23; 508(3): 438–42.
25. Norris KA, Schrimpf JE, Flynn JL, Morris SM Jr. Enhance- ment of macrophage microbicidal activity: supplemental arginine and citrulline augment nitric oxide production in murine perito- neal macrophages and promote intracellular killing of Trypano- soma cruzi. Infect Immun 1995; 63: 2793–6.
26. Osowska S. Citrulline increases arginine pools and restores nitrogen balance after massive intestinal resection. Gut 2004; 53(12): 1781–6.
27. Osowska S, Duchemann T, Walrand S, Paillard A, Boirie Y, Cynober L, Moinard C. Citrulline modulates muscle protein metab- olism in old malnourished rats. Am J Physiol Endocrinol Metab 2006; 291: E582–E586.
28. Wiśniewski J, Fleszar MG, Piechowicz J, et al. A novel mass spectrometry-based method for simultaneous determination of asymmetric and symmetric dimethylarginine, l-arginine and l-citrulline optimized for LC-MS-TOF and LC-MS/MS. Biomed Chromatogr 2017; 31(11).
29. European Medicines Agency: Guideline on Bioanalytical Method Validation, https://www.ema.europa.eu/en/documents/scientific-guideline/guideline-bioanalytical-method-validation_en.pdf, 2021.
30. World Medical Association Declaration of Helsinki: ethical principles for medical research involving human subjects. Jama 2013; 310(20): 2191–4.
31. Evans JD. Straightforward statistics for the behavioral sciences. Pacific Grove: Brooks/Cole Pub. Co., 1996.
32. Douda L, Vokurková D, Douda T, et al. Memory B lymphocytes in peripheral blood in coeliac disease: a pilot study. Gastroenterologie a hepatologie 2019; 73(4): 296–302.
33. Salmi TT, Collin P, Korponay-Szabó IR, et al. Endomysial antibody-negative coeliac disease: clinical characteristics and intestinal autoantibody deposits. Gut 2006; 55(12): 1746–53.
34. Lebwohl B, Michaëlsson K, Green PHR, Ludvigsson JF. Persistent Mucosal Damage and Risk of Fracture in Celiac Disease. J Clin Endocrinol Metab 2014; 99(2): 609–16.
35. Windmueller HG, Spaeth AE. Source and fate of circulating citrulline. Am J Physiol. 1981; 241(6): E473–80.
36. Hoffenberg EJ. Another measurement of the elusive entity called "intestinal function". J Pediatr Gastroenterol Nutr 2003; 37(3): 325.
37. Curis E, Crenn P, Cynober L. Citrulline and the gut. Curr Opin Clin Nutr Metab Care 2007; 10(5): 620–6.
38. Papadia C, Sherwood RA, Kalantzis C, et al. Plasma citrulline concentration: a reliable marker of small bowel absorptive capacity independent of intestinal inflammation. Am J Gastroenterol 2007; 102(7): 1474–82.
39. Miceli E, Poggi N, Missanelli A, Bianchi P, Moratti R, Corazza GR. Is serum citrulline measurement clinically useful in coeliac disease? Intern Emerg Med 2008; 3(3): 233-6.
40. Oliverius M, Kudla M, Baláz P, Valsamis A. [Plasma citrulline concentration – a reliable noninvasive marker of functional enterocyte mass]. Cas Lek Cesk 2010; 149(4): 160–2.
41. Fragkos KC, Forbes A. Citrulline as a marker of intestinal function and absorption in clinical settings: A systematic review and meta-analysis. United European Gastroenterol J 2018; 6(2): 181–91.
42. Breuillard C, Cynober L, Moinard C. Citrulline and nitrogen homeostasis: an overview. Amino Acids 2015; 47(4): 685–91.
43. Couchet M, Pestour S, Breuillard C, et al. Regulation of citrulline synthesis in human enterocytes: Role of hypoxia and inflammation. Biofactors 2022; 48(1): 181–9.
44. Blachier F, Darcy-Vrillon B, Sener A, Duée PH, Malaisse WJ. Arginine metabolism in rat enterocytes. Biochim Biophys Acta 1991; 1092: 304–10.
45. Bahri S CE, Aussel C. Caractérisation in vitro du transport instestinal de la citrulline. Nut Clin Metab 2006: 111.
46. Cynober L. Pharmacokinetics of arginine and related amino acids. J Nutr 2007; 137(6 Suppl 2): 1646s–9s.
47. Rabier D, Kamoun P. Metabolism of citrulline in man. Amino Acids 1995; 9(4): 299–316.
48. Curis E, Nicolis I, Moinard C, et al. Almost all about citrulline in mammals. Amino Acids 2005; 29(3): 177–205.
49. Rogers G, Winter B, McLaughlan C, Powell B, Nesci T. Peptidy-larginine deiminase of the hair follicle: characterization, localization, and function in keratinizing tissues. J Invest Dermatol 1997; 108: 700–7.
50. Ishida-Yamamoto A, Senshu T, Takahashi H, Akiyama K, Nomura K, Iizuka H Decreased deiminated keratin K1 in psoriatic hyper-proliferative epidermis. J Invest Dermatol 2000; 114: 701–5.
51. Moscarello MA, Pritzker L, Mastronardi FG, Wood DD Peptidy-larginine deiminase: a candidate factor in demyelinating disease. J Neurochem 2002; 81: 335–43.
52. Nicholas AP, Sambandam T, Echols JD, Tourtellotte WW. Increased citrullinated glial fibrillary acidic protein in secondary progressive multiple sclerosis. J Comp Neurol 2004; 473: 128–36.
53. Asaga H, Yamada M, Senshu T. Selective deimination of vimentin in calcium ionophore-induced apoptosis of mouse peritoneal macro-phages. Biochem Res Commun 1998; 243: 641–6.
54. Girbal-Neuhauser E, Durieux JJ, Arnaud M, et al. The epitopes targeted by the rheumatoid arthritis- associated antifilaggrin autoantibodies are posttranslationally generated on various sites of (Pro) filaggrin by deimination of arginine residues. J Immunol 1999; 162: 585–94.
55. Sivashanmugam M, Jaidev J, Umashankar V, Sulochana KN. Ornithine and its role in metabolic diseases: An appraisal. Biomed Pharmacother 2017; 86: 185–94.
56. Hozyasz KK, Szaflarska-Popławska A, Ołtarzewski M, et al. [Whole blood citrulline levels in patients with coeliac disease]. Pol Merkur Lekarski 2006; 20(116): 173–5.

57. Mandel H, Levy N, Izkovitch S, Korman SH. Elevated plasma citrulline and arginine due to consumption of Citrullus vulgaris (watermelon). J Inherit Metab Dis 2005; 28(4): 467–72.
58. Wang T, Steel G, Milam AH, Valle D. Correction of ornithine accumulation prevents retinal degeneration in a mouse model of gyrate atrophy of the choroid and retina. Proc Natl Acad Sci U S A 2000; 97(3): 1224–9.
59. Barilli A, Rotoli BM, Visigalli R, Dall'Asta V. Gliadin activates arginase pathway in RAW264.7 cells and in human monocytes. Biochim Biophys Acta 2014; 1842(9): 1364–71.

Risk Factors for Candidemia in Intensive Care Unit: A Matched Case Control Study from North-Western India

Ekadashi Rajni, Ashish Jain, Shilpi Gupta*, Yogita Jangid, Rajat Vohra

ABSTRACT

Candidemia is one of the significant causes of mortality amongst critically ill patients in Intensive Care Units (ICUs). This study aimed to assess the incidence, risk factors and antifungal susceptibility pattern in candidemia cases admitted in ICU in a tertiary care hospital in Jaipur, Rajasthan from June 2021 to November 2021. *Candida* species isolated from blood culture of clinically suspected patients of sepsis were defined as candidemia cases. Blood culture and antifungal susceptibility testing were performed as per standard laboratory protocol. Analyses of risk factors was done between candidemia cases and matched controls in a ratio of 1 : 3. Forty-six candidemic cases and 150 matched controls were included in the study. *C. tropicalis* was the most prevalent species (22/46; 48%) followed by *C. auris* (8/46; 17%) and *C. albicans* (7/46; 15%). *Candida* species showed good sensitivity to echinocandins (97%) followed by amphotericin B (87%) and voriconazole (80%). In multivariate analysis, longer stay in ICU, presence of an indwelling device, use of immunosuppressive drugs and positive SARS-CoV-2 infection were associated with increased risk of candidemia. The constant evaluation of risk factors is required as prediction of risks associated with candidemia may help to guide targeted preventive measures with reduced morbidity and mortality.

KEYWORDS

candidemia; invasive candidiasis; antifungal susceptibility; ICU; risk factors

AUTHOR AFFILIATIONS

Mahatma Gandhi Medical University and Science Technology, Riico Institutional Area, Sitapura, Tonk Road, Jaipur, Rajasthan, India

* Corresponding author: Mahatma Gandhi Medical University and Science Technology, Riico Institutional Area, Tonk Rd, Sitapura, Jaipur, Rajasthan – 302020, India; e-mail: shilpigupta15nov@yahoo.com

Received: 29 July 2022
Accepted: 11 November 2022
Published online: 2 February 2023

Acta Medica (Hradec Králové) 2022; 65(3): 83–88
https://doi.org/10.14712/18059694.2022.23

INTRODUCTION

The last few decades have witnessed an unprecedented level of development in the healthcare industry. Both the therapeutic and diagnostic facilities have grown multi-fold, making saving lives a reality (1). The flip side to this development is there is an increased number of patients in intensive care units battling immunosuppression, either because of the disease itself or because of the potent broad-spectrum drugs and critical procedures being used (2, 3). All this has led to a humungous burden of patients at risk of invasive fungal infections. Bloodstream infections (BSIs) caused by *Candida* species have become a substantial threat in the hospital and are associated with high morbidity and mortality (4).

The profile of species involved in candidemia is continuously evolving and novel species are being described. Non *albicans candida* (NAC) are being isolated more frequently as compared to *C. albicans* (5). While *C. albicans* is being reported more frequently in the developed countries, *C. tropicalis* and *C. parapsilosis* dominate the epidemiology in developing nations (3, 6). *C. auris*, first described in 2009, has currently spread in several continents and is frequently associated with nosocomial infections and outbreaks. The resistance profile of *C. auris* and the high mortality associated with *C. auris* infections present quite a challenge for physicians. An increasing level of antifungal resistance to commonly used first and second-line antifungals is being observed on a global level (7, 8). Traditionally, invasive candidiasis has been associated with immunocompromised and chronic inflammatory states. The use of broad-spectrum antibiotics, recent surgery and indwelling central venous catheters (CVC), particularly those for total parenteral nutrition and prolonged hospital stay are known to be the other risk factors associated with candidemia (9).

Most of this data is limited by the fact that the large majority of studies have been retrospective in nature. Given the geographical variation and evolving epidemiology of candidemia, it is important to determine the predictors of candidemia in any particular set up (4). Also, a fresh perspective is needed to assess these factors in the light of currently pursuing pandemic. With this background the present matched case control study was conducted to assess the prevalence, risk factors and antifungal susceptibility pattern in invasive candidemia cases from medico-surgical intensive care unit (MS-ICU) of our hospital.

MATERIALS AND METHODS

STUDY DESIGN, SETTINGS AND DATA COLLECTION

This single center matched case control observational study was conducted in a 1450 bedded tertiary care teaching hospital in Jaipur, Rajasthan from June 2021 to November 2021. Patients above 18 years of age with at least one blood culture positive for Candida spp. were included as cases in the study. The cases and controls were matched in a ratio of 1 : 3. The matching criteria included gender, admission in the ICU at about the same time as the candidemia patients and SOFA score of at least 5, at the day of admission in ICU.

The data concerning demographics (age, sex), comorbidities, length of ICU stay, presence of any indwelling device, use of steroids or chemotherapeutic drugs, presence of COVID 19 infection, laboratory tests (CRP, procalcitonin) and outcome was collected daily by dedicated nurses on a predesigned proforma and compiled on excel sheet for both cases and controls. Initial pilot study was done on 30 patients for the validation of proforma. After the successful completion of pilot study, all 196 study participants were assessed using this clinical proforma.

DEFINITION

All blood culture results of suspected sepsis cases during the study period at our centre were screened for candidemia cases. Candidemia was defined as the isolation of *Candida* sp. from at least one blood culture in patients with clinical signs and symptoms suggestive of sepsis. For patients with multiple positive blood culture, only the first case of candidemia was included, and furthermore a new episode of candidemia was defined if the duration between the two episodes was more than 30 days (4).

MICROBIOLOGICAL ANALYSIS

Blood culture was performed using automated blood culture system BactecTM FX (Becton Dickinson, Sparks, MD). Identification was done using VITEK-2 automated system (bioMèrieux, Marcy-l'Étoile, France) with VITEK 2 (YST) cards. *Candida* isolates that could not be identified conclusively by VITEK-2 were subjected to matrix-assisted laser desorption ionization- time of flight mass spectrometry (MALDI-TOF MS; Bruker Biotyper OC version 3.1, Daltonics, Bremen, Germany) using an ethanol formic acid extraction protocol. Antifungal susceptibility was performed using the broth microdilution assay according to the Clinical and Laboratory Standards Institute guidelines (10).

ETHICAL APPROVAL

Approval of the Institutional Ethics Committee was obtained prior to the commencement of this study (MGMC&H/IEC/JPR/2021/552).

STATISTICAL ANALYSIS

The data was entered in a Microsoft excel worksheet. The qualitative data was assessed using Chi-square test while quantitative data was assessed using t test for both cases and control group. P value less than 0.05 was considered as statistically significant.

RESULTS

Out of 811 blood cultures that tested positive during the study period, candidemia was detected in 46, incidence being 5.7%. Thereafter, these 46 cases of candidemia and 150 matched controls were included in the study. The median age (and IQR) was found to 52 (39–58) for candidemia cases and 51 (38–65) for non-candidemia patients.

Tab. 1 Invitro susceptibility profile of various *Candida* species against the antifungals tested.

Candida isolates (N = 46)	Azoles		Echinocandins			AMB Sensitive N (%)	Flucytosine Sensitive N (%)
	Fluconazole Sensitive N (%)	Voriconazole Sensitive N (%)	Anidulafungin Sensitive N (%)	Caspofungin Sensitive N (%)	Micafungin Sensitive N (%)		
Candida tropicalis (22)	20 (91%)	21 (96%)	22 (100%)	20 (91%)	22 (100%)	22 (100%)	21 (96%)
Candida auris (8)	0	2 (25%)	7 (88%)	8 (100%)	8 (100%)	2 (25%)	1 (13%)
Candida albicans (7)	7 (100%)	7 (100%)	7 (100%)	7 (100%)	7 (100%)	7 (100%)	6 (86%)
Candida parapsilosis (4)	3 (75%)	2 (50%)	4 (100%)	4 (100%)	4 (100%)	4 (100%)	4 (100%)
Candida famata (2)	2 (100%)	2 (100%)	2 (100%)	2 (100%)	2 (100%)	2 (100%)	2 (100%)
Candida glabrata (2)	NA	2 (100%)	2 (100%)	2 (100%)	2 (100%)	2 (100%)	1 (50%)
Candida lusitaniae (1)	1 (100%)	1 (100%)	1 (100%)	0	0	1 (100%)	1 (100%)

AMB – Amphotericin B

The distribution of various *Candida* species isolated from blood culture is shown in figure 1. *C. tropicalis* was the most common isolated *Candida* sp. (22/46; 48%) followed by *C. auris* (8/46; 17%) and *C. albicans* (7/46; 15%). Table 1 shows the antifungal susceptibility pattern to various antifungals tested. *C. albicans* isolates were 100% sensitive to almost all antifungals except for 5-flucytosine (5-FC) which showed resistance in 14% (1/7) of the isolates. Amongst the NAC, maximum resistance was seen against fluconazole (11/39; 28%) followed by voriconazole (9/39; 23%) and 5-flucytosine (9/39; 23%). *C. auris* was found to be most resistant speciesamongst all with 75–88% resistance against azoles, amphotericin B and 5-FC.

A summary of clinico-demographic characteristics of cases and matched controls is presented in Table 2. The univariate comparison (candidemia vs non-candidemia patients), longer stay in ICU for more than 20 days (39% vs 12%), presence of central venous catheter (61% vs 17%), raised C reactive protein (CRP) levels (76% vs 7%) and presence of SARS-CoV-2 infection (15% vs 1%) were associated with the development of candidemia. Hypertension, diabetes and chronic lung disease were the most common comorbidities associated with patients admitted in the ICU in both case and control groups and were not found to be statistically significant in development of candidemia. All patients who developed candidemia (46/46; 100%) were on immunosuppressants and was found to be statistically significant risk factor in comparison to the control group (61/150; 41%). Almost all patients had previous history of exposure to broad spectrum antibiotics in previous 30 days and 9 (9/46; 19.6%) patients had history of empirical use of antifungal drug in past 90 days (data not shown in table). The overall, mortality rate was found to be 28% in candidemia patients and did not show any statistical correlation when compared to non-candidemia (36%) patients.

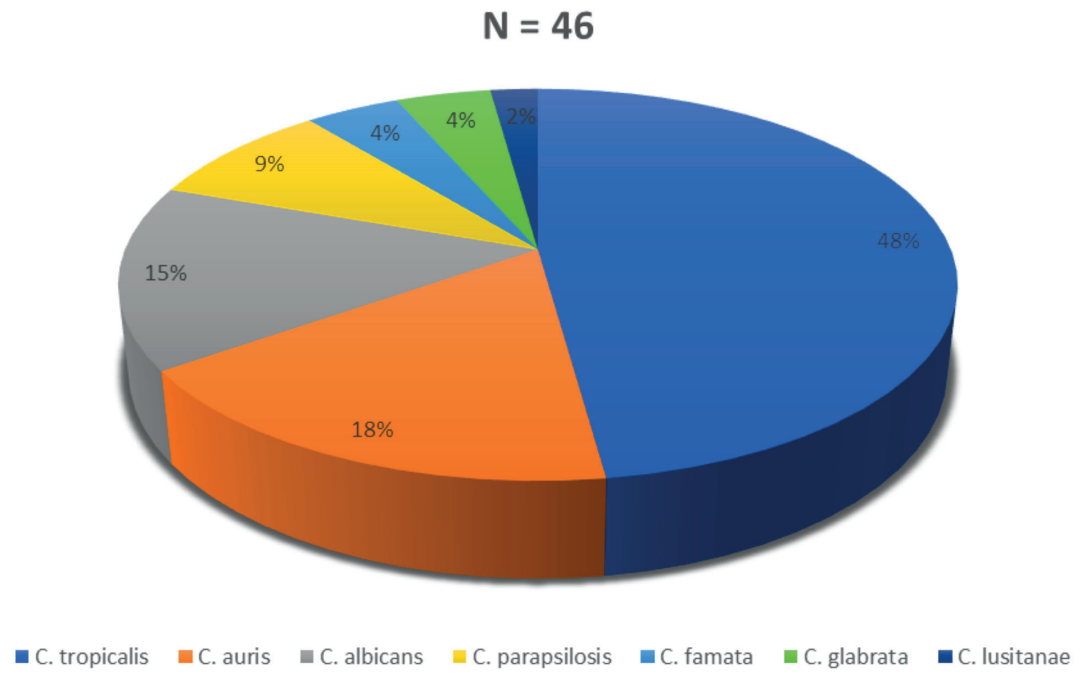

Fig. 1 Distribution of *Candida* species isolated from blood culture.

Tab. 2 Clinico-demographic characteristics of patients with and without candidemia.

Variables		Patients with candidemia (N = 46) (%)	Patients without candidemia (N = 150) (%)	Chi square (df)	p value
Age	≤ 60 ≥ 61	38 (83) 8 (17)	91 (61) 59 (39)	7.533 (1)	0.006
Gender	Male	30 (65)	97 (65)	0.012 (1)	0.914
Gender **Duration of hospital stay**	Female	16 (35)	53 (35)	0.012 (1) 15.520 (1)	0.914 < 0.0001
	< 20 days	28 (61)	132 (88)		
Duration of hospital stay **Presence of indwelling device**	≥ 20 days	18 (39)	18 (12)	15.520 (1) 26.751 (3)	< 0.0001 < 0.0001
	CVC	27 (61)	25 (17)		
Presence of indwelling device **Comorbidities**	Mechanical ventilation	37 (80)	77 (51)	26.751 (3) 11.543 (6)	< 0.0001 0.073
	Urinary catheter	43 (94)	126 (84)		
	Dialysis line/drains	3 (7)	44 (29)		
	Hypertension	11 (24)	49 (33)		
Comorbidities **C Reactive Protein (Positive)**	Diabetes	11 (24)	55 (37)	11.543 (6) 92.031 (1)	0.073 < 0.0001
	Lung disease	13 (28)	49 (33)		
	Renal disease	3 (12)	46 (31)		
	Liver disease	1 (2)	13 (9)		
	Malignancy	5 (11)	19 (13)		
	History of previous surgery	0	26 (17)		
	Yes	35 (76)	10 (7)		
C Reactive Protein (Positive) **Procalcitonin (Positive)**	No	11 (24)	140 (93)	92.031 (1) 13.338 (1)	< 0.0001 < 0.0001
	Yes	15 (33)	14 (9)		
Procalcitonin (Positive) **Use of steroids/immunosuppressive drugs**	No	31 (67)	136 (91)	13.338 (1) 47.630 (1)	< 0.0001 < 0.0001
	Yes	46 (100)	61 (41)		
Use of steroids/immunosuppressive drugs **History of COVID 19 infection**	No	0	89 (59)	47.630 (1) 15.503 (1)	< 0.0001 < 0.0001
	Yes	7 (15)	1 (1)		
History of COVID 19 infection **Final disease outcome**	No	39 (89)	149 (99)	15.503 (1) 0.088 (1)	< 0.0001 0.766
	Deceased	13 (28)	48 (32)		
Final disease outcome	Survived	33 (72)	102 (68)	0.088 (1)	0.766

df – degree of freedom; CVC – Central venous catheter

DISCUSSION

The present study provides an insight into the current epidemiology of candidemia in an adult ICU of a tertiary care teaching hospital in Jaipur with the incidence rate of 5.7%. A multicentric observational study conducted nationwide at 27 ICUs documented an overall incidence of 6.51 cases/1,000 ICU admission (4). This variation may be due to the timing of our observation which is done during pandemic era while the previous mentioned Indian data is from pre-pandemic period. Routsi et al., and several other researchers have observed that the incidence of candidemia increased significantly during the COVID-19 pandemic in comparison to pre-COVID era (11). More than three-fourth of the patients (83%) with candidemia were more than 60 years of age similar to most other studies (5, 12). Invasive candidiasis is not directly related to the virulence of the pathogen rather attributed to the subsidence of the host immune system. Thus, increased incidence in ICUs is encountered due to various factors including age related comorbidities which accentually compromise defence mechanism in patients enhancing chances of *Candida* invasion (5, 9).

The present study observed that NAC (85%) outnumbered *C. albicans* (15%). The steadily increased occurrence of NAC in comparison to *C. albicans* in ICU settings has been documented in various Indian as well as in western literature in the past few years. This shift has been attributed to rampant use of fluconazole which has led to selection and increased survival of resistant strains (13, 14, 16). According to a review on epidemiology of invasive candidiasis incidence of NAC has increased and *C. albicans* has decreased worldwide though distribution of candida species is variable region wise. As documented by same review

the incidence of C. glabrata is high in USA while most frequently observed species in Asia-Pacific countries and Latin America are *C. tropicalis* and *C. parapsilosis* (2). Amongst NAC, the predominant *Candida* species in our study was *C. tropicalis* (48%) followed by *C. auris* (17%). It is interesting to note that observation on candidemia from the same setting during August 2020 to Jan 2021 had shown *C. auris* being the most common isolate. The study highlighted the fact of anticipation of *C. auris* outbreak during COVID-19 pandemic, which was documented worldwide (7).

It is an important observation to note that the earlier study on candidemia was conducted during the first pandemic wave in our country while the present study was conducted after the decline of second wave wherein epidemiology of candidemia seems to be shifting back steadily to the pre-pandemic period. The sudden increase in frequency of *C. auris* in ICU during COVID pandemic waves is multifactorial. It is attributed to mainly rampant and irrational use of steroids, broad-spectrum antibiotics and breach in infection control practices which contributed to sudden widespread of *C. auris* amongst patients where this species was already prevalent in hospital environment (15). This finding is in contrast to studies reported from other parts of the world including European countries where still *C. albicans* is the predominant species in ICU even during the ongoing pandemic (6, 9, 16).

In concordance with other studies across the country, we observed an overall higher invitro resistance in NAC isolates compared to *C. albicans* (7, 17, 18). Azoles including fluconazole showed 100% susceptibility against *C. albicans* thus implying it can be used as drug of choice in our ICU settings. The present study documents a high degree of antifungal resistance amongst *C. auris* isolates, a fact which has been apprised in previous studies from our centre (3, 7).

In our cohort, *C. auris* strains (n = 8) were resistant to azoles (75–100%), 75% and 88% were resistant to AMB and flucytosine respectively. Minimal resistance was shown against anidulafungin (13%) while sparing other echinocandins (Table 2). *C. auris* is known for its unfavourable antifungal susceptibility profile with most of the isolates being multi drug resistant. Implementation of adequate infection control measures and continuous surveillance remain the mainstay to prevent colonization of *C. auris* in a way to reduce development of invasive candidiasis rather treating the MDR strain (8).

The traditional risk factors associated with candidemia known since decades are characterised under demographic factors, co-morbid conditions, medical interventions and usage of broad-spectrum antibiotics and steroids (6). A systematic review had identified 29 risk factors extracted from 34 studies worldwide for invasive candidiasis. This review highlights significant association with comorbid conditions especially HIV and use of invasive devices. Other important risk factors with strong odds ratio, documented were patients on broad-spectrum antibiotics, total parenteral nutrition and previous *Candida* colonization (19).

Several studies in literature can be searched which have evaluated the risk factors for development of candidemia. However, majority of them were conducted on specific patient cohorts and did not use case control design. The present study used matched case-control methodology to identify multiple risk factors associated with candidemia in the critical care unit. Overall, the present study confirmed the strong association with increased length of ICU stay, presence of invasive devices, use of steroids and COVID-19 infection in comparison to patients who did not develop candidemia (p value < 0.001) (Table 2) which is in sync with other studies (6, 20). A sudden upsurge in candidemia cases ranging from two to upto ten folds have been noted during and after COVID 19 pandemic all over the globe (7, 21, 22). In an analysis by Rouitsi et al., the risk factors for severe COVID-19 disease and development of candidemia are almost similar (11). However, the commonest risk factor for increased incidence of candidemia in COVID-19 patients being the rampant use of antimicrobials empirically for suspected as well as for confirmed secondary bacterial infections which was stressed upon by various studies (7, 11, 23).

While evaluating candidemia cases it was found that markers of systemic inflammation like C reactive protein (CRP) was increased in majority of cases (35/46; 76%) while levels of procalcitonin (PCT) were increased only in 33% (15/46) cases. An interesting finding by Yin et al., among immunocompromised children have suggested that high CRP and low PCT levels help to differentiate invasive fungal infection from bacterial blood stream infection which is in favour with our findings. However, further studies with larger data in adults are required to establish this fact taking time of testing also under consideration (24).

The mortality rate found in our study was found to be 28.3% which is slightly lower than the previously reported studies (35–80%). This could possibly due to the fact that all the patients included in our study were not critically ill as suggested by low SOFA score during time of admission (9). Invasive devices constitute an important and unavoidable part of patient care. At the same time, they have an undisputed role to play in the genesis of nosocomial infections. They are invariably found to be the nidus of infection in patients requiring critical care (2, 4). Repeated and religious reinforcement is required for infection control practices including strict compliance to hand hygiene. The five moments of hand hygiene as endorsed by WHO must be adhered to. Also, a culture of "device intolerance" needs to be developed as propounded by Gopal P (25).

The strength of our study lies in its prospective matched case control design, taking care of many confounding variables along with collection of a sufficient amount of information to properly model potential risk factors of candidemia. Also, biochemical parameters like CRP and procalcitonin have been included as potential factors influencing the situation, thus enlarging the domain of risk factors studied.

However, there are certain limitations of the study which need to be brought forth. The correlation of few important risk factors like *Candida* score, correlation of candidemia cases with exact duration and specific class of antimicrobial use have been missed. Further studies on continuous surveillance of patients admitted in critical care for *Candida* colonization should be undertaken to establish its role in development of invasive candidiasis.

CONCLUSION

C. tropicalis followed by *C. auris* were the most frequently isolated candida species from candidemia patients in critical care unit. Age group more than 50 years, longer stay in ICU, presence of an indwelling device, use of steroids or immunosuppressive drugs and presence of SARS-CoV-2 infection were significant risk factors associated with candidemia patients in comparison to the control group. The continuous change in epidemiology and emergence of acquired resistance to antifungals necessitate regular monitoring to develop local guidelines for strengthening antifungal stewardship. Constant evaluation of risk factors in any particular set up is mandated to help intensivists to assess distribution and trends of candidemia.

ACKNOWLEDGEMENTS

The authors thank Dr Anuradha Chowdhary, Professor, Department of Medical Mycology, Vallabhbhai Patel Chest Institute, Delhi, for contributing in identification of isolates by MALDI-TOF MS and antifungal susceptibility testing. Additionally, she provided valuable suggestions for this manuscript.

REFERENCES

1. Dasgupta S, Das S, Chawan NS, Hazra A. Nosocomial infections in the intensive care unit: incidence, risk factors, outcome and associated pathogens in a public tertiary teaching hospital of Eastern India. Indian J Crit Care Med 2015; 19: 14–20.
2. Yapar N. Epidemiology and risk factors for invasive candidiasis. Ther Clin Risk Manag 2014 Feb 13; 10: 95–105.
3. Rajni E, Chaudhary P, Garg VK, Sharma R, Malik M. A complete clinico-epidemiological and microbiological profile of candidemia cases in a tertiary-care hospital in Western India. Antimicrobial Stewardship & Healthcare Epidemiology. Cambridge University Press 2022; 2(1): e37.
4. Chakrabarti A, Sood P, Rudramurthy SM, et al. Incidence, characteristics and outcome of ICU-acquired candidemia in India. Intensive Care Med 2015; 41(2): 285–95.
5. Ahmad S, Kumar S, Rajpal K, et al. Candidemia Among ICU Patients: Species Characterisation, Resistance Pattern and Association with Candida Score: A Prospective Study. Cureus 2022; 14(4): e24612.
6. Poissy J, Damonti L, Bignon A, et al. Risk factors for candidemia: a prospective matched case-control study. Crit Care 2020; 24(1): 109.
7. Rajni E, Singh A, Tarai B, et al. A High Frequency of Candida auris Blood Stream Infections in Coronavirus Disease 2019 Patients Admitted to Intensive Care Units, Northwestern India: A Case Control Study. Open Forum Infect Dis 2021; 8(12): ofab452.
8. Briano F, Magnasco L, Sepulcri C, et al. Candida auris Candidemia in Critically Ill, Colonized Patients: Cumulative Incidence and Risk Factors. Infect Dis Ther 2022; 11(3): 1149–60.
9. Xiao Z, Wang Q, Zhu F, An Y. Epidemiology, species distribution, antifungal susceptibility and mortality risk factors of candidemia among critically ill patients: a retrospective study from 2011 to 2017 in a teaching hospital in China. Antimicrob Resist Infect Control 2019; 8: 89.
10. Clinical and Laboratory Standards Institute. Reference Method for Broth Dilution Anti–Fungal Susceptibility Testing of Yeasts. CLSI Document M27. 4th ed. Wayne, PA: Clinical and Laboratory Standards Institute 2017.
11. Routsi C, Meletiadis J, Charitidou E, et al. Epidemiology of Candidemia and Fluconazole Resistance in an ICU before and during the COVID-19 Pandemic Era. Antibiotics 2022; 11: 771.
12. Tortorano AM, Peman J, Bernhardt H, et al.: Epidemiology of candidaemia in Europe: results of 28-month European Confederation of Medical Mycology (ECMM) hospital-based surveillance study. Eur J Clin Microbiol Infect Dis 2004; 23: 317–22.
13. Giri S, Kindo AJ, Kalyani J. Candidemia in intensive care unit patients: a one year study from a tertiary care center in South India. J Postgrad Med 2013; 59(3): 190–5.
14. Kaur H, Singh S, Rudramurthy SM, et al. Candidaemia in a tertiary care centre of developing country: Monitoring possible change in spectrum of agents and antifungal susceptibility. Indian J Med Microbiol 2020; 38(1): 110–6.
15. Chowdhary A, Sharma A. The lurking scourge of multidrug resistant Candida auris in times of COVID-19 pandemic. J Glob Antimicrob Resist 2020; 22: 175–6.
16. Macauley P, Epelbaum O. Epidemiology and Mycology of Candidaemia in non-oncological medical intensive care unit patients in a tertiary center in the United States: Overall analysis and comparison between non-COVID-19 and COVID-19 cases. Mycoses 2021; 64(6): 634–40.
17. Sabhapandit D, Lyngdoh WV, Bora I, Prasad A, Debnath K, Elantamilan D. Prevalence of non-albicans candidemia in a tertiary-care hospital in Northeast India. Int J Med Sci Public Health 2017; 6: 1620–5.
18. Kothari A, Sagar V. Epidemiology of candida bloodstream infections in a tertiary care institute in India. Indian J Med Microbiol 2009; 27(2): 171–2.
19. Thomas-Rüddel DO, Schlattmann P, Pletz M, Kurzai O, Bloos F. Risk Factors for Invasive Candida Infection in Critically Ill Patients: A Systematic Review and Meta-analysis. Chest 2022; 161(2): 345–55.
20. Li D, Xia R, Zhang Q, Bai C, Li Z, Zhang P. Evaluation of candidemia in epidemiology and risk factors among cancer patients in a cancer center of China: an 8-year case-control study. BMC Infect Dis 2017; 17(1): 536.
21. Nucci M, Barreiros G, Guimaraes LF, Deriquehem VAS, Castineiras AC, Nouer SA. Increased incidence of candidemia in a tertiary care hospital with the COVID-19 pandemic. Mycoses 2021; 64: 152–6.
22. Riche CVW, Cassol R, Pasqualotto AC. Is the frequency of candidemia increasing in COVID-19 patients receiving corticosteroids? J Fungi 2020; 6: 286.
23. Segala FV, Bavaro DF, Di Gennaro F, et al. Impact of SARS-CoV-2 Epidemic on Antimicrobial Resistance: A Literature Review. Viruses 2021; 13: 2110.
24. Liu Y, Zhang X, Yue T, et al. Combination of C-Reactive Protein and Procalcitonin in Distinguishing Fungal from Bacterial Infections Early in Immunocompromised Children. Antibiotics 2022; 11(6): 730.
25. Gopal P. Providencial Progression: Time tobe Intolerant. Indian J Crit Care Med 2022; 26(4): 409–10.

The Choroid after Half-Dose Photodynamic Therapy in Chronic Central Serous Chorioretinopathy

Evita Evangelia Christou[1,*], Andreas Katsanos[1], Ilias Georgalas[2], Vassilios Kozobolis[3], Christos Kalogeropoulos[1], Maria Stefaniotou[1]

ABSTRACT

Purpose: To characterize choroidal structure and vasculature after half-dose verteporfin photodynamic therapy (hd-vPDT) in eyes with chronic central serous chorioretinopathy using Enhanced Depth Imaging Optical Coherence Tomography (EDI OCT) and Optical Coherence Tomography Angiography (OCT-A).

Methods: This prospective case-control study included 10 eyes. Choroid was examined before and at 1 month following hd-vPDT. We measured choroidal thickness (CT) at subfoveal area and at 750 μm nasal and temporal of fovea and thickness of Haller and choriocapillaris/Sattler layers. Whole (WA), luminal (LA) and interstitial area (IA) at EDI-OCT, and perfusion density at OCT-A were analyzed. The unaffected fellow eyes were used for comparisons.

Results: Mean CT at subfoveal area and at 750 μm nasal and temporal of fovea, values of Haller and choriocapillaris/Sattler layers and those of WA, LA and IA were reduced, while PD increased at 1 month after hd-vPDT (all $p < 0.001$). There was a significant ($p < 0.05$) negative correlation ($\rho = -0.658$) between PD and post-treatment logMARVA. None of analyzed parameters reached values of unaffected fellow eye.

Conclusion: Following hd-vPDT, choroidal thickness with both luminal and interstitial components markedly decreased, while perfusion of choriocapillaris improved.

KEYWORDS

chronic central serous chorioretinopathy; half-dose photodynamic therapy; enhanced depth imaging; optical coherence tomography; optical coherence tomography angiography; PDT

AUTHOR AFFILIATIONS

[1] Department of Ophthalmology, Faculty of Medicine, School of Health Sciences, University of Ioannina, Ioannina, Greece
[2] First Department of Ophthalmology, General Hospital of Athens G. Gennimatas, Medical School, National and Kapodistrian University of Athens, Greece
[3] Department of Ophthalmology, Faculty of Medicine, School of Health Sciences, University of Patras, Patras, Greece
* Corresponding author: University of Ioannina, Faculty of Medicine, Stavrou Niarchou Avenue, 45500, Ioannina, Greece; email: evitachristou@gmail.com

Received: 11 May 2022
Accepted: 14 November 2022
Published online: 2 February 2023

Acta Medica (Hradec Králové) 2022; 65(3): 89–98
https://doi.org/10.14712/18059694.2022.24

INTRODUCTION

Central serous chorioretinopathy (CSC) is a chorioretinal disorder characterized by accumulation of fluid under the neurosensory retina due to dysfunction of the retinal pigment epithelium (RPE) (1–4). A multimodal imaging approach has proposed that CSC in fact belongs to the pachychoroid spectrum of disorders, and the choroidal vascular hyperpermeability is the main pathophysiological feature (5–8). Novel techniques have provided new insights in the visualization of the choroidal structure and circulation. Optical Coherence Tomography using the Enhanced Depth Imaging (EDI-OCT) mode allows us to highlight increased choroidal thickness and dilated large vessels in CSC (9–13). Optical Coherence Tomography Angiography (OCT-A) provides detailed information regarding the retinal and choroidal vascular layers and is useful for the analysis of perfusion changes (6, 7, 14, 15). The use of depth-resolved imaging methods provides evidence of the pathogenic mechanism of CSC during the course of the disease and after treatment (8–15). Verteporfin photodynamic therapy (vPDT) for the treatment of chronic cases has been proven to be an efficacious option. It has been successfully used to reduce choroidal vascular congestion and hyperpermeability (16–19). Recent studies have reported safety-enhanced protocols, in an attempt to minimize potential complications of standard vPDT such as choroidal ischemia, retinal pigment epithelium atrophy, choroidal neovascularization (CNV). Indeed, half-dose or low-fluence modified protocols have been found to be effective and safe in anatomical and functional outcomes regarding resolution of subretinal fluid (SRF), visual acuity (VA) and choroidal perfusion (20, 21).

The aim of this prospective study was to perform a quantitative analysis of choroidal structure including luminal and interstitial components and to analyze vascular changes of the choriocapillaris (CC) before and after applying half-dose vPDT (hd-vPDT) in patients with chronic CSC.

MATERIAL AND METHODS

STUDY DESIGN

The study was conducted at the Department of Ophthalmology of the University of Ioannina, Greece, between September 2020 and March 2021 after receiving approval from the institutional ethics committee (gm 3/24N2020). The investigation adhered to the tenets of the Declaration of Helsinki. Informed consent was obtained from each patient before any study-related activity.

This was a prospective comparative study. Patients who underwent hd-vPDT for chronic CSC were recruited and their data were analyzed. Inclusion criteria were: a) diagnosis of chronic CSC, b) a single successful treatment with hd-vPDT, c) complete EDI-OCT and OCT-A data before vPDT (at baseline within 1 week from treatment) and at 1 month post-treatment. Eyes with a history of previous ocular surgery other than uncomplicated phacoemulsification, trauma, high refractive errors, co-existent macular and vitreoretinal pathology were excluded to avoid potential confounding effects. In addition, we excluded eyes that had previously received any form of therapy (vPDT, laser photocoagulation, intravitreal injections of anti-vascular endothelial growth factor/VEGF) or those with evidence of CNV secondary to CSC. Patients with low quality images were also excluded. The patients' unaffected fellow eyes were used for comparisons.

All participants underwent a comprehensive eye examination that included measurement of best corrected visual acuity, determination of intraocular pressure, slit-lamp biomicroscopy and fundus examination after pupil dilation. The indication for applying vPDT was chronic CSC with persistent SRF of at least 3 months duration and foveal involvement that was confirmed by active angiographic leakage in fluorescein angiography and choroidal vascular hyperpermeability in indocyanine green angiography. EDI-OCT and OCT-A imaging were performed at baseline and at 1 month after treatment.

EDI-OCT AND OCT-A IMAGING PROTOCOLS

SD-OCT (Cirrus HD-OCT, Zeiss, Jena, Germany) using the eye-tracking system was performed to investigate the choroidal area. The scans were acquired with the EDI mode at baseline and at 1 month after applying vPDT. Choroidal thickness (CT) was measured at the subfoveal area and at 750 μm to the nasal and temporal sides of the fovea. The Haller's layer and the Sattler's/CC layer were assessed independently. Choroidal layer analysis of the OCT images were manually performed based on previously described methods (22). Choroidal thickness measurements were performed using as landmarks the distance from the outer portion of the hyper-reflective line which corresponds to the Bruch's membrane, and the inner hyper-reflective line of the choroid-sclera interface. The cut-off size of the large choroidal vessels in the horizontal images through the fovea was selected at 100 μm. Choroidal vessels located closest to the center of the fovea having a diameter larger than 100 μm were used for the measurements. The latter defined the horizontal line from the innermost point of the large choroidal vessels that intersected the subfoveal CT measurement line perpendicularly. The subfoveal choroidal large vessel layer thickness was defined as the distance from the point of intersection on the subfoveal CT line to the inner surface of the sclera. The thickness of the Sattler's/CC layer was derived by subtracting the thickness of the Haller's layer from the subfoveal CT. All EDI-OCT images were imported in Image J. A 1500 μm wide area under the fovea (750 μm nasally and temporally to the center) extending vertically from the RPE to the chorioscleral border was selected for analysis. The scans were thresholded by an Otsu method and analyzed by binarization technique (7, 14). The white zones corresponded to the interstitial spaces and the black zones to the luminal area. The whole area (WA), luminal area (LA) and interstitial area (IA) of the choroid were calculated. A ratio between luminal part and total choroid corresponding to the choroidal vascularity index (CVI) in former studies was measured (23). The measurements for the images were obtained by the same examiner. All images were obtained at approximately 10 am to avoid the influence of diurnal choroidal changes.

OCT-A generates high-resolution three-dimensional maps of the retinal and choroidal microvasculature. Imaging was performed with the AngioPlex® OCT Angiography (ZEISS, Jena, Germany), and OCT angiograms were acquired in a 6 × 6 mm scan pattern automatically centered at the fovea. En face images of the CC plexus were generated and automated layer segmentation was performed by the software using a slab between 29 and 49 µm below the RPE reference. The automated slab segmentation was checked and manually corrected in case of inaccuracy. Each OCT angiogram at the CC layer was imported in Image J for analysis. Binarization of the images was made by the Otsu method, which is an automatic threshold selection from gray-level histograms. Contrary to the EDI-OCT scans, the white zones corresponded to the lumen of vessels of the CC network and the black zones to the interstitial area. We assumed that the percentage of white zones was an indirect measure of the choroidal vascular flow area of the CC, therefore the percentage area occupied by the microvasculature in the CC layer defined the perfusion density. Indeed, a ratio between luminal part and total area in the CC layer was equivalent to the vascular density in previous studies (14). All scans were reviewed to ensure their quality was sufficient.

HALF-DOSE VPDT PROTOCOL

The participants were subjected to the modified protocol of hd-vPDT. Verteporfin was administrated intravenously at a dose of 3 mg/m² over 10 minutes. Fifteen minutes after the initial verteporfin infusion, the treatment area was exposed to a delivery of diode laser of 689 nm with a fluence of 600 mw/cm² for 83 seconds and total laser energy of 50 J/cm² using a contact lens (Volk Area Centralis). The spot size had a diameter of 1000 µm larger than the greatest linear dimension of the choroidal exudation in indocyanine green angiography (ICGA). Patients were advised to avoid exposure to sunlight for 48 h post-treatment due to a potential risk of skin photosensitivity.

STATISTICAL METHODOLOGY

We performed the statistical analysis using SPSS version 25.0 (SPSS Inc., Chicago, IL, USA). Continuous variables were expressed as mean ± standard deviation (SD). We used the paired t-test for normally distributed data, or the Mann-Whitney U test for non-normally distributed data. To examine the correlation of two continuous variables, we used the Pearson coefficient for normally distributed data, or the Spearman coefficient for non-normally distributed data. Normality was tested using the Shapiro-Wilks test. For all tests, statistical differences were determined to be significant at $p < 0.05$.

RESULTS

We examined 17 patients (19 eyes) with chronic CSC. After exclusion criteria a total of ten eyes of 10 patients (8 men, 2 women) who underwent hd-PDT were included in the study. We excluded 2 eyes with residual SRF at first month after treatment, 2 eyes with evidence of CNV, 3 eyes which had received previous treatment (1 with vPDT, 2 with anti-VEGF injections) and a patient with systemic contraindications to verteporfin. The mean age of the patients was 44.70 ± 5.72 years (range: 37–56). The mean period between diagnosis of CSC and applying treatment was 22.40 ± 3.20 months (range: 18–29). All eyes included in the analysis had complete resolution of SRF at 1 month post-treatment. We analyzed the EDI-OCT and OCT-A characteristics at baseline and at 1 month after hd-vPDT. The patients' descriptive characteristics expressed in mean ± SD are shown in table 1.

EDI-OCT CHOROIDAL VALUES

The measurements of the CT at the subfoveal area and at 750 µm nasal and temporal of the center after treatment were significantly lower compared to those before (all $p < 0.001$). Moreover, treated eyes at baseline had signifi-

Tab. 1 Descriptive characteristics of affected and unaffected fellow eyes. Data presented as mean ± standard deviation.

	affected before PDT	affected after PDT	unaffected fellow
SFCT (µm)	411.50 ± 34.74	307.30 ± 17.96	297.30 ± 19.60
750N CT (µm)	375.60 ± 33.53	290.40 ± 18.33	280.60 ± 16.81
750TCT (µm)	391.00 ± 33.21	299.10 ± 18.68	288.50 ± 17.60
Haller (µm)	329.20 ± 38.80	215.30 ± 15.84	202.20 ± 17.65
CC+Sattler (µm)	82.30 ± 16.89	92.00 ± 18.01	95.70 ± 18.06
EDI-OCT whole area (mm²)	944197.00 ± 37291.06	684814.50 ± 25568.83	666526.50 ± 17657.02
EDI-OCT luminal area(mm²)	649590.10 ± 36586.50	288724.90 ± 25281.89	464548.50 ± 20683.03
EDI-OCT interstitial area(mm²)	294606.90 ± 19163.4	196089.60 ± 31901.30	201978.00 ± 22301.40
CVI (%)	0.69 ± 0.02	0.71 ± 0.04	0.70 ± 0.03
perfusion (%)	48.29 ± 1.89	50.56 ± 1.75	51.27 ± 1.57
visual acuity (logMAR)	0.56 ± 0.23	0.49 ± 0.25	0.14 ± 0.05

Abbreviations: PDT – photodynamic therapy; SFCT – subfoveal choroidal thickness; CT – choroidal thickness; EDI-OCT – enhanced depth imaging optical coherence tomography; CVI – choroidal vascularity index

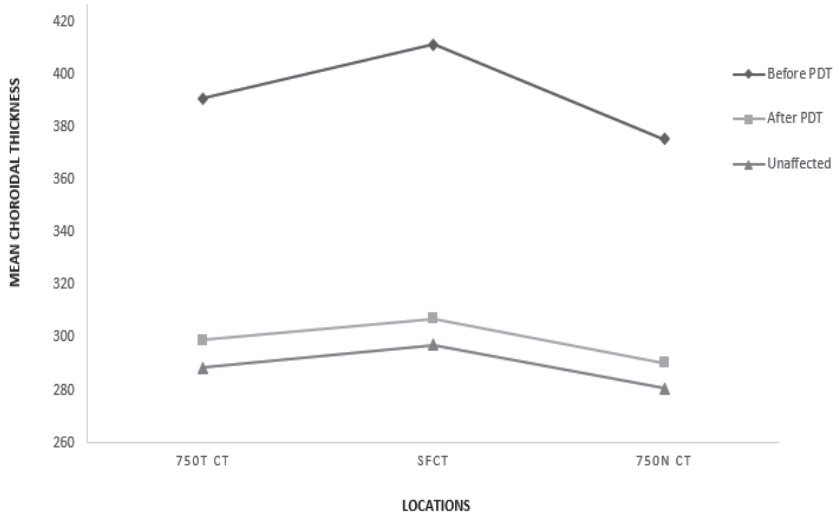

Fig. 1 Choroidal thickness values in affected eyes before and after photodynamic therapy (PDT) and in fellow eyes.

Legend 1: Mean subfoveal choroidal thickness (SFCT) and mean choroidal thickness at 750µm temporal (750T CT) and nasal (750N CT) of the fovea. Mean values before PDT: SFCT = 411.50, 750N CT = 375.60, 750T CT = 391.00; after PDT: SFCT = 307.30, 750N CT = 290.40, 750T CT = 299.10; unaffected fellow: SFCT = 297.30, 750N CT = 280.60, 750T CT = 288.50; $p \leq 0.001$ in all cases.

cantly higher measurements of the CT at each region compared to the fellow eyes (all $p < 0.001$), while after treatment the measurements remained higher than those of the contralateral eye (all $p < 0.001$) (Figure 1). After vPDT, the thickness of Haller's and CC/Sattler's layers was significantly lower compared to those before treatment (all $p < 0.001$). Moreover, treated eyes at baseline had significantly higher measurements of the choroidal layers compared to the fellow eyes (all $p < 0.001$), while after treatment the thickness measurements of Haller's and CC/Sattler's remained higher than those of the contralateral eye ($p = 0.005$ and $p < 0.001$, respectively) (Figure 2). The binarized EDI-OCT images indicated markedly lower values of the total area of the choroid, as well as the luminal and interstitial components after treatment compared to baseline (all $p < 0.001$). In addition, treated eyes at baseline had markedly higher values of WA, LA, and IA compared to the fellow eyes (all $p < 0.001$). Following vPDT, the values remained higher than those of the contralateral eyes (all $p < 0.001$) (Figure 3). Regarding the CVI, the mean values before vPDT did not differ significantly compared to those following treatment ($p = 0.148$). CVI of treated eyes before vPDT did not differ statistically from that of the fellow eyes ($p = 0.491$). The mean values of CVI post-treatment were significantly higher than those of the fellow eyes ($p = 0.043$).

OCT-A CC VALUES

The values of the perfusion at the CC layer following vPDT were significantly higher compared to those before treatment ($p < 0.001$). Moreover, treated eyes before vPDT had statistically significant lower values of the CC perfusion compared to the fellow eyes ($p < 0.001$), while the post-treatment values did not reach the level of the contralateral eye ($p < 0.001$) (Figure 4).

VISUAL OUTCOMES

Visual outcomes after vPDT significantly improved compared to pre-treatment measurements ($p = 0.039$). However, the post-treatment VA did not reach the level of the contralateral eye ($p = 0.005$). Correlation analyses revealed that both pre-treatment and post-treatment VA correlated in a significantly negative way to the perfusion values of the CC ($p = 0.028$ and $p = 0.038$, respectively) (Figure 5).

DISCUSSION

Herein, we report microstructural and microcirculation changes in eyes with chronic CSC after applying hd-vPDT. Using a morphometric analysis of binarized EDI-OCT B-scans and en face OCT angiograms, we evaluated vascular and stromal alterations of the total choroidal area and flow changes of the CC network at 1 month post-treatment. It has been largely demonstrated that modified safety-enhanced treatment protocols are efficient in the amelioration of functional outcomes and the restoration of retinal architecture. Indeed, vPDT with a reduced dose of verteporfin or a shortened time of laser emission still achieve satisfactory treatment efficacy with a diminished hypoxic effect on choroidal circulation (20, 21). In the study by Chan et al. (8), the potential of a temporary short-term CC hypoperfusion followed by vascular remodeling and improvement of blood circulation over time has been speculated. Histopathologically, occlusion of the CC has been observed in human eyes 1 week post-vPDT followed by vascular recanalization (24), while reperfusion in the normal choroid may occur within 7 weeks (25). The introduction of novel depth-resolved imaging modalities, including the techniques of EDI-OCT and OCT-A, has provided new insights in the visualization of the chorioretinal morphology and microcirculation. A number of series have revealed variability in qualitative and quantitative analyses of flow pattern, luminal and interstitial components and perfusion evaluated during the post-treatment follow-up period (9–15). Changes in the choroid, and specifically the CC plexus, may indicate the treatment impact on choroidal tissue remodeling and imply the potential of anatomical and functional recovery (6–15).

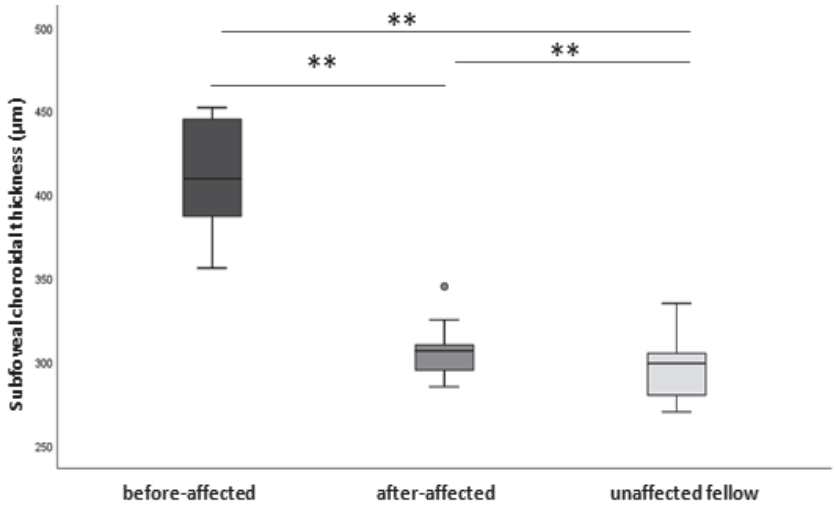

Fig. 2a Subfoveal choroidal thickness values in affected and fellow eyes.

Legend 2a: Means plot Subfoveal choroidal thickness (µm) from affected eyes (before-affected, after-affected) and fellow eyes (unaffected fellow). Mean values SFCT: before PDT = 411.50, after PDT = 307.30, unaffected fellow = 297.30, **p<0.001.

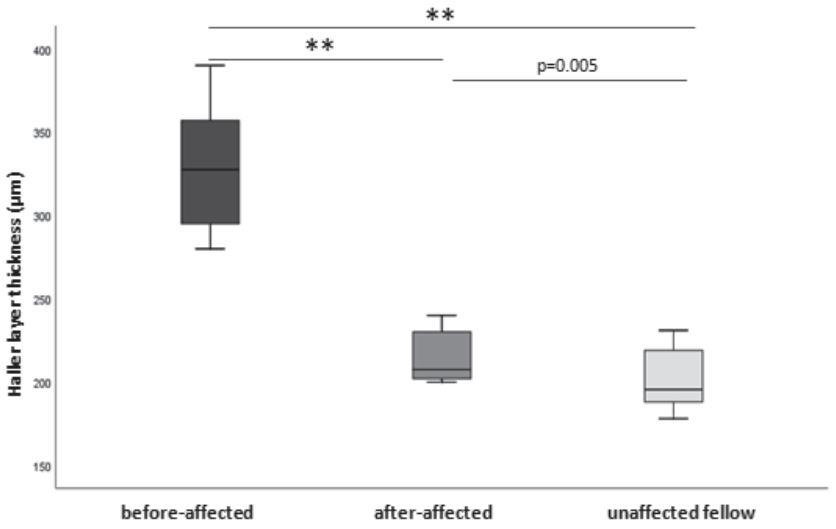

Fig. 2b Haller layer thickness values in affected and fellow eyes.

Legend 2b: Means plot Haller layer thickness (µm) from affected eyes (before-affected, after-affected) and fellow eyes (unaffected fellow). Mean values Haller: before PDT = 329.20, after PDT = 215.30, unaffected fellow = 202.20, **p < 0.001.

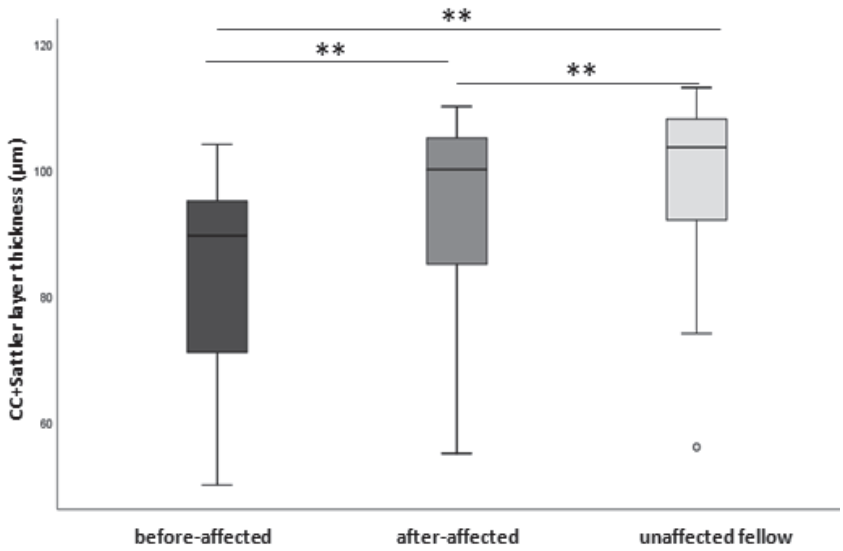

Fig. 2c Choriocapillaris (CC) + Sattler layer thickness values in affected and fellow eyes.

Legend 2c: Means plot Choriocapillaris (CC) + Sattler layer thickness (µm) from affected eyes (before-affected, after-affected) and fellow eyes (unaffected fellow). Mean values CC+Sattler: before PDT = 82.30, after PDT = 92.00, unaffected fellow = 95.70, **p < 0.001

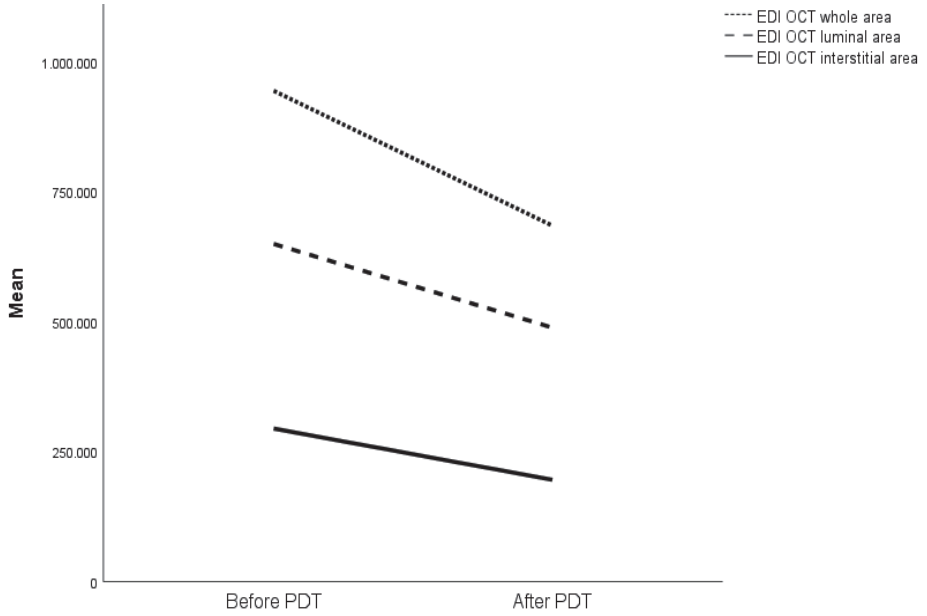

Fig. 3a Choroidal area at enhanced depth imaging Optical Coherence Tomography (EDI-OCT) in affected eyes before and after photodynamic therapy (PDT).

Legend 3a: Change of mean choroidal area (whole, luminal and interstitial) in affected eyes before and after PDT. Mean values whole: before PDT = 994197.00, after PDT = 684814.50, unaffected fellow = 666526.50; luminal: before PDT = 649590.10, after PDT = 288724.90, unaffected fellow = 464548.50; interstitial: before PDT = 294606.90, after PDT = 196089.60, unaffected fellow = 201978.00; $p \leq 0.001$ in all cases.

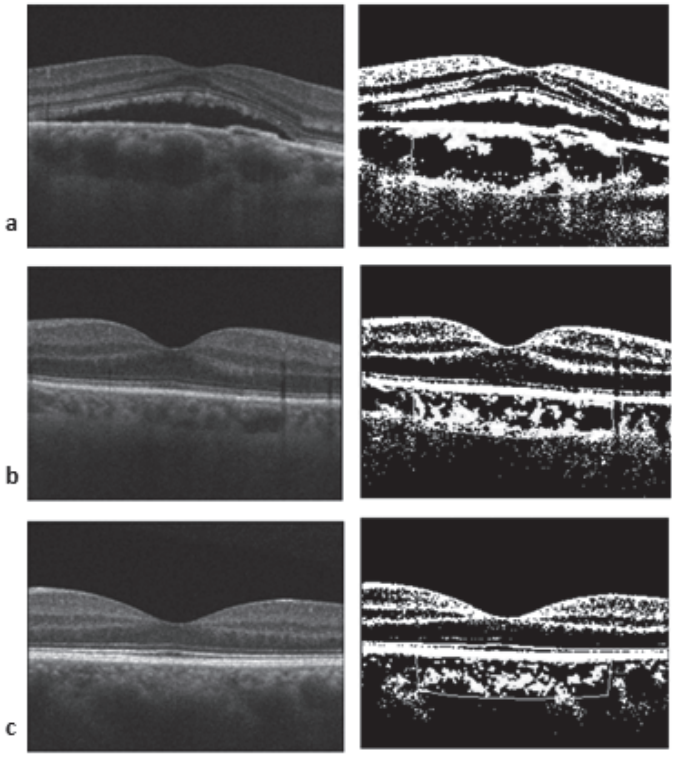

Fig. 3b EDI-OCT images of affected and fellow eye.

Legend 3b: a) EDI-OCT image (left) and binarized image (right) of affected eye before PDT, b) EDI-OCT image (left) and binarized image (right) of affected eye after PDT, c) EDI-OCT image (left) and binarized image (right) of unaffected fellow eye.

In the present study, we investigated the functional and anatomic outcomes occurring after hd-vPDT, focusing especially on the choroidal vasculature. Our results indicated changes regarding the choroidal structure components after treatment. The values of CT at each measured area (subfoveal, 750μm nasally as well as temporally off the center) using EDI-OCT were significantly decreased at 1 month after vPDT compared to those before treatment, as previously described. However, the CT of the affected eye even after vPDT was higher than that of the contralateral eye. Indeed, the comparison of the CT measurements on both eyes of patients with unilateral disease at a 12-month follow-up period has indicated that the CT in vPDT-treated eyes remained thicker than that of the contralateral eye (26, 27), with the amount of choroidal thinning being significantly greater after full-fluence vPDT as compared to modified protocols (28). Authors of previous studies have commented that choroidal thinning following vPDT should be considered in the context of normalization of the pathologically increased choroid, and that the treatment effect does not go beyond the remodeling process, and therefore does not lead to choroidal atrophy (29). Of note, concerning measurements of Haller and CC/Sattler layer thickness, our results support a significant decline in both layers post-treatment. Regarding the thickness of individual choroidal layers, the existing evidence does not unequivocally specify which layers are most affected: some papers have only documented the decrease of total choroidal thickness (20, 27, 28), while others have found a decrease of individual layers (9, 13, 21).

We further examined the whole choroidal area and its components using the binarization process. The reduction of WA we found in our study may reflect the decrease in CT. Previous publications have reported shrinkage of the total choroidal volume with controversial outcomes concerning the luminal and stromal components (9–13). A reduction of the luminal part may confirm the hypothesis

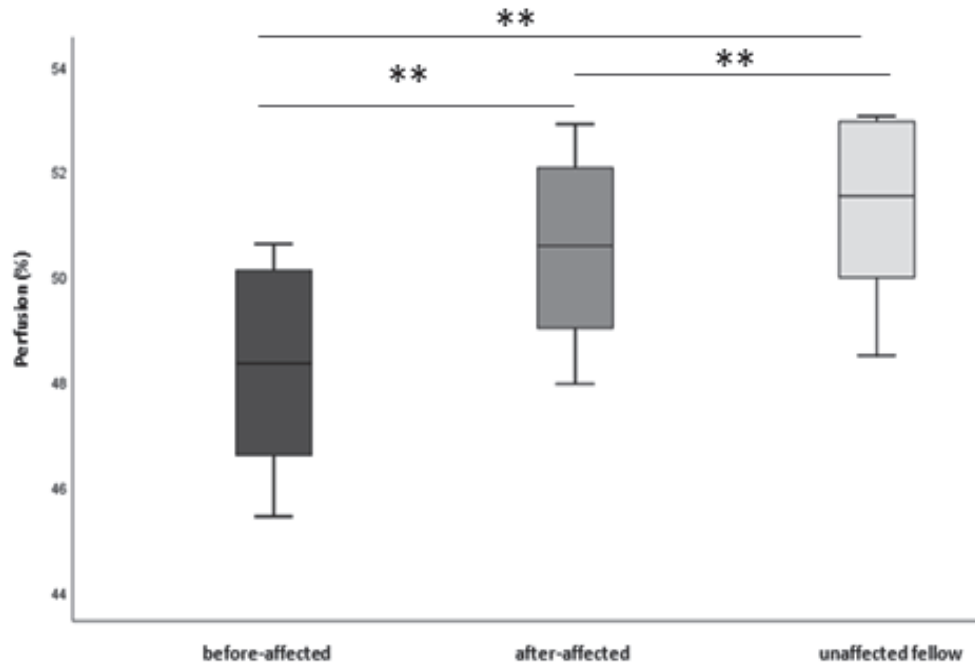

Fig. 4a Perfusion values in affected and fellow eyes.

Legend 4a: Means plot perfusion (%) from affected eyes (before-affected, after-affected) and fellow eyes (unaffected fellow). Mean values perfusion: before PDT = 48.29, after PDT = 50.56, unaffected fellow = 51.27, **p < 0.001.

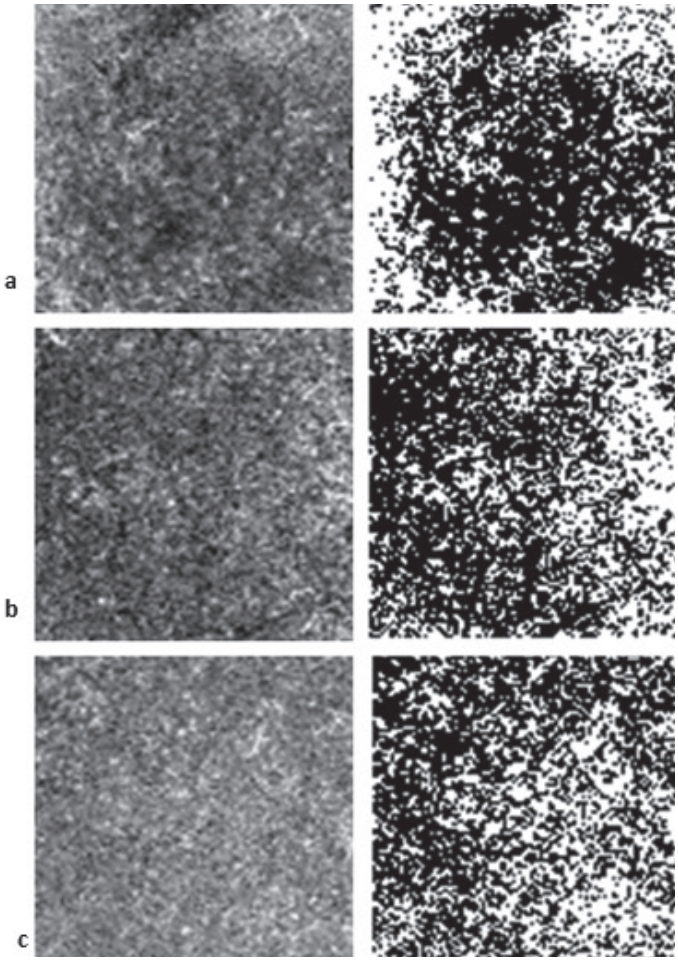

Fig. 4b OCT-A images of affected and fellow eye.

Legend 4b: a) OCT-A image (left) and binarized image (right) of affected eye before PDT, b) OCT-A image (left) and binarized image (right) of affected eye after PDT, c) OCT-A image (left) and binarized image (right) of unaffected fellow eye.

that vPDT has a direct effect on large choroidal vessels as the main treatment target, which results in decongestion of CC vessels and eventual vascular flow re-establishment with a secondary modification on CC compression and vascular flow amelioration. Apart from the significant reduction of the vascular luminal area, our study demonstrated a simultaneous reduction of the interstitial part. The decrease of both choroidal vascular and extravascular components implies that the effect of vPDT on choroidal tissue may involve vascular decongestion as well as interstitial fluid absorption. The CVI is a novel parameter to quantitatively describe the choroidal vasculature demonstrating the ratio of LA over WA (23). In our study, both LA and WA were reduced after vPDT treatment, thus offering a potential explanation why CVI did not markedly differ compared to that at baseline.

Our analysis of OCT angiograms by the binarization method has mainly focused on the perfusion changes of the CC layer following vPDT. The flow pattern and vascular perfusion changes have been initially analyzed in a qualitative way followed by further precise quantification (30–34). Previous studies have mentioned an aberrant flow pattern at the CC layer in eyes before receiving vPDT with a tendency to recovery and a relatively uniform flow after the absorption of SRF at 1 month post-treatment, just as in our study (30–32, 34). Contrary to these results, Teussink et al (6) mentioned an aberrant CC vasculature that persisted even after the absorption of SRF, and appeared to be independent of the therapy used. This discrepancy among the results of these studies may be due to the difference in the period between the provided treatment and the OCT-A examination. Teussink and co-authors (6) may have missed any primary therapeutic effect seen on OCT-A. On the other hand, studies lacking long-term follow-up would have not confirmed a potential recurrent

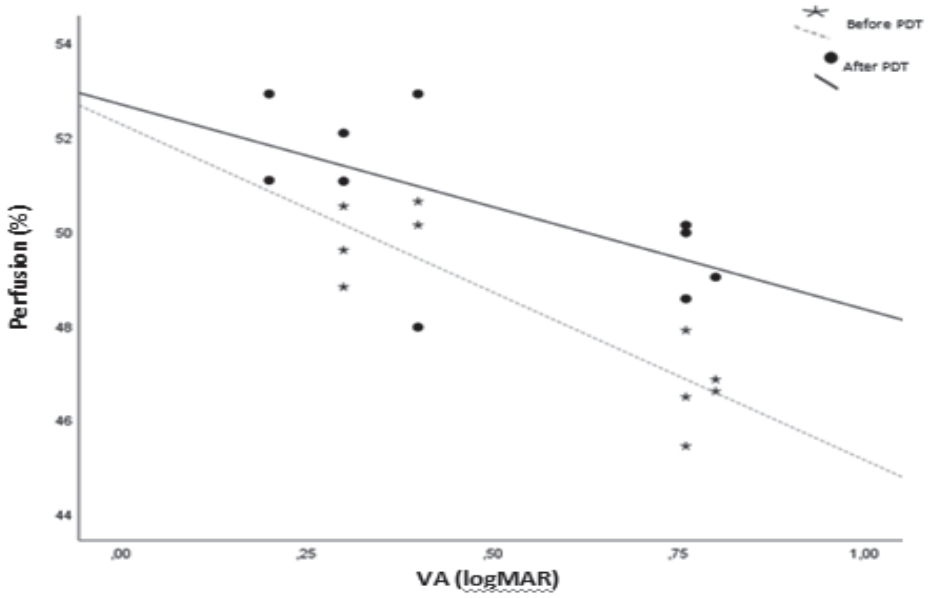

Fig. 5 Correlation analysis between perfusion and visual acuity (VA) before and after photodynamic therapy (PDT) in affected eyes.
Legend 5: Significantly negative correlation between perfusion and VA before and after PDT in affected eyes (before PDT: $\rho = -0.688$, $p = 0.028$; after PDT: $\rho = -0.658$, $p = 0.038$).

the compression on the CC layer. In fact, the overexpression of VEGF at the treatment site due to potential tissue hypoxia may consequently contribute to an increase in vascular density in deep capillary plexus and CC related to the process of recovery. The restoration of the latter vascular networks that constitute the main nutrient and oxygen supply of photoreceptors, leads to resultant photoreceptor recovery and visual acuity improvement (36). Analyzing the OCT angiograms by the binarization method in our study, the percentage area occupied by the microvasculature in specific regions defined the perfusion density. Consequently, our results support the hypothesis that the recovery of CC perfusion leads to photoreceptor restoration, which is in turn associated with functional improvement.

To date, there is limited evidence for the association between CC perfusion changes and VA after vPDT in patients with CSC. We consider this information highly relevant for clinical practice, as perfusion changes could possibly serve as a predicting factor for visual outcomes. Our study contributes to a little-studied issue which undoubtedly warrants further investigation. Certain limitations of the current study need to be considered. Firstly, our patients were examined at only one time-point after vPDT. Obviously, any short-term changes may have been missed. In addition, our results may not accurately portray the choroidal vascular and structural characteristics over the long-term. We intend to follow our patients in order to detect further morphometrical and functional changes over time. Secondly, the sample size was relatively small. Nonetheless, even this small sample enabled the detection of significant differences in several of the investigated parameters. Conceivably, more subtle effects could have been detected using a larger sample. Thirdly, the patients' fellow unaffected eyes were used as controls. One could suggest that contralateral eyes of patients with CSC should not be considered normal, as differences have been found when compared to healthy controls (37). However, using different participants as controls could also be problematic, as the eyes of different people me have important physiological differences. In addition, we should not ignore the intrinsic limitations of the imaging technology used. It can be argued for instance, that a swept-source system would be more appropriate than a spectral-domain device for the visualization of the CC and the choroidal area. On the other hand, it was recently shown that both swept-source and spectral-domain systems are comparable for choroidal measurements (38). Lastly, it should be noted that our results were produced using a well-known image-processing software and a procedure (binarization) that has been used for similar studies (7, 13, 14, 31, 34, 39). Theoretically, employing different imaging platforms and processes could have produced different results.

CONCLUSION

EDI-OCT and OCT-A improves our knowledge on the pathophysiology of choroidal circulation and morphologic changes induced by hd-vPDT in chronic CSC. Quantification of choroidal components may highlight the anatomic response of the tissue to treatment with hd-vPTD. The increase of perfusion density in OCT angiographic findings following treatment may signify functional improvement.

DECLARATIONS

All authors meet the International Committee of Medical Journal Editors (ICMJE) criteria for authorship for this article, take responsibility for the integrity of the work as a whole, and have given their approval for this version to be published.

COMPETING INTERESTS

Andreas Katsanos has to report lecture fees and congress expenses by Santen, Vianex, Zwitter and research grant by Laboratoires Thea. The other authors have no disclosures to report.

FUNDING

No funding or sponsorship was received for this study.

DATA AVAILABILITY

All data will be available upon reasonable request.

REFERENCES

1. Prünte C, Flammer J. Choroidal capillary and venous congestion in central serous chorioretinopathy. Am J Ophthalmol 1996 Jan; 121(1): 26–34.
2. Katsanos A, Gorgoli K, Konidaris V, Empeslidis T. An overview of risk factors, diagnosis and treatment of central serous chorioretinopathy. In: Patrick Evans (Ed). Central serous chorioretinopathy (CSCR): risk factors, diagnosis and management. Chapter 1, p: 1–32. Nova Science Publishers Inc, NY, USA, 2017.
3. Piccolino FC, de la Longrais RR, Ravera G, et al. The foveal photoreceptor layer and visual acuity loss in central serous chorioretinopathy. Am J Ophthalmol 2005 Jan; 139(1): 87–99.
4. Spaide RF, Campeas L, Haas A, et al. Central serous chorioretinopathy in younger and older adults. Ophthalmology 1996 Dec; 103(12): 2070–9; discussion 2079–80.
5. Cheung CMG, Lee WK, Koizumi H, Dansingani K, Lai TYY, Freund KB. Pachychoroid disease. Eye (Lond) 2019 Jan; 33(1): 14–33.
6. Teussink MM, Breukink MB, van Grinsven MJ, et al. OCT Angiography Compared to Fluorescein and Indocyanine Green Angiography in Chronic Central Serous Chorioretinopathy. Invest Ophthalmol Vis Sci 2015 Aug; 56(9): 5229–37.
7. Sonoda S, Sakamoto T, Yamashita T, et al. Choroidal structure in normal eyes and after photodynamic therapy determined by binarization of optical coherence tomographic images. Invest Ophthalmol Vis Sci 2014 Jun 3; 55(6): 38939. Erratum in: Invest Ophthalmol Vis Sci 2014 Aug; 55(8): 4811–2.
8. Chan WM, Lam DS, Lai TY, Tam BS, Liu DT, Chan CK. Choroidal vascular remodelling in central serous chorioretinopathy after indocyanine green guided photodynamic therapy with verteporfin: a novel treatment at the primary disease level. Br J Ophthalmol 2003 Dec; 87(12): 1453–8.
9. Flores-Moreno I, Arcos-Villegas G, Sastre M, Ruiz-Medrano J, Arias-Barquet L, Duker JS, Ruiz-Moreno JM. Changes in choriocapillaris, sattler, and haller layer thicknesses in central serous chorioretinopathy after half-fluence photodynamic therapy. Retina 2020 Dec; 40(12): 2373–8.
10. Hua R, Liu L, Li C, Chen L. Evaluation of the effects of photodynamic therapy on chronic central serous chorioretinopathy based on the mean choroidal thickness and the lumen area of abnormal choroidal vessels. Photodiagnosis Photodyn Ther 2014 Dec; 11(4): 519–25.
11. Razavi S, Souied EH, Cavallero E, Weber M, Querques G. Assessment of choroidal topographic changes by swept source optical coherence tomography after photodynamic therapy for central serous chorioretinopathy. Am J Ophthalmol 2014 Apr; 157(4): 852-60.
12. Chung YR, Kim JW, Kim SW, Lee K. Choroidal thickness in patients with central serous chorioretinopathy: Assessment of Haller and Sattler Layers. Retina 2016 Sep; 36(9): 1652–7.
13. Izumi T, Koizumi H, Maruko I, et al. Structural analyses of choroid after half-dose verteporfin photodynamic therapy for central serous chorioretinopathy. Br J Ophthalmol 2017 Apr; 101(4): 433–7.
14. Nicolò M, Rosa R, Musetti D, Musolino M, Saccheggiani M, Traverso CE. Choroidal Vascular Flow Area in Central Serous Chorioretinopathy Using Swept-Source Optical Coherence Tomography Angiography. Invest Ophthalmol Vis Sci 2017 Apr 1; 58(4): 2002–10.
15. Chan SY, Wang Q, Wei WB, Jonas JB. Optical coherence tomographic angiography in central serous chorioretinopathy. Retina 2016 Nov; 36(11): 2051–8.
16. Taban M, Boyer DS, Thomas EL, Taban M. Chronic central serous chorioretinopathy: photodynamic therapy. Am J Ophthalmol 2004 Jun; 137(6): 1073–80.
17. Silva RM, Ruiz-Moreno JM, Gomez-Ulla F, et al. Photodynamic therapy for chronic central serous chorioretinopathy: a 4-year follow-up study. Retina 2013 Feb; 33(2): 309–15.
18. Yannuzzi LA, Slakter JS, Gross NE, et al. Indocyanine green angiography-guided photodynamic therapy for treatment of chronic central serous chorioretinopathy: a pilot study. 2003. Retina 2012 Feb; 32 Suppl 1: 288–98.
19. Tsakonas GD, Kotsolis AI, Koutsandrea C, Georgalas I, Papaconstantinou D, Ladas ID. Multiple spots of photodynamic therapy for the treatment of severe chronic central serous chorioretinopathy. Clin Ophthalmol 2012; 6: 1639–44.
20. Reibaldi M, Cardascia N, Longo A, et al. Standard-fluence versus low-fluence photodynamic therapy in chronic central serous chorioretinopathy: a nonrandomized clinical trial. Am J Ophthalmol 2010 Feb; 149(2): 307–315.e2.
21. Ma DJ, Park UC, Kim ET, Yu HG. Choroidal vascularity changes in idiopathic central serous chorioretinopathy after half-fluence photodynamic therapy. PLoS One 2018 Aug 27; 13(8): e0202930.
22. Branchini LA, Adhi M, Regatieri CV, et al. Analysis of choroidal morphologic features and vasculature in healthy eyes using spectral-domain optical coherence tomography. Ophthalmology 2013 Sep; 120(9): 1901–8.
23. Iovino C, Pellegrini M, Bernabei F, et al. Choroidal Vascularity Index: An In-Depth Analysis of This Novel Optical Coherence Tomography Parameter. J Clin Med 2020 Feb 21; 9(2): 595.
24. Schlötzer-Schrehardt U, Viestenz A, Naumann GO, Laqua H, Michels S, Schmidt-Erfurth U. Dose-related structural effects of photodynamic therapy on choroidal and retinal structures of human eyes. Graefes Arch Clin Exp Ophthalmol 2002 Sep; 240(9): 748-57.
25. Husain D, Kramer M, Kenny AG, et al. Effects of photodynamic therapy using verteporfin on experimental choroidal neovascularization and normal retina and choroid up to 7 weeks after treatment. Invest Ophthalmol Vis Sci 1999 Sep; 40(10): 2322–31.
26. Schmidt-Erfurth U, Laqua H, Schlötzer-Schrehard U, Viestenz A, Naumann GO. Histopathological changes following photodynamic therapy in human eyes. Arch Ophthalmol 2002 Jun; 120(6): 835–44.
27. Maruko I, Iida T, Sugano Y, Furuta M, Sekiryu T. One-year choroidal thickness results after photodynamic therapy for central serous chorioretinopathy. Retina 2011 Oct; 31(9): 1921–7.
28. Oh BL, Yu HG. Choroidal thickness after full-fluence and half-fluence photodynamic therapy in chronic central serous chorioretinopathy. Retina 2015 Aug; 35(8): 1555–60.
29. Kim YK, Ryoo NK, Woo SJ, Park KH. Choroidal Thickness Changes After Photodynamic Therapy and Recurrence of Chronic Central Serous Chorioretinopathy. Am J Ophthalmol 2015 Jul; 160(1): 72–84.e1.
30. Demircan A, Yesilkaya C, Alkin Z. Early choriocapillaris changes after half-fluence photodynamic therapy in chronic central serous chorioretinopathy evaluated by optical coherence tomography angiography: Preliminary results. Photodiagnosis Photodyn Ther 2018 Mar; 21: 375–8.
31. Demirel S, Özcan G, Yanık Ö, Batıoğlu F, Özmert E. Vascular and structural alterations of the choroid evaluated by optical coherence tomography angiography and optical coherence tomography after half-fluence photodynamic therapy in chronic central serous chorioretinopathy. Graefes Arch Clin Exp Ophthalmol 2019 May; 257(5): 905–12.
32. Chan SY, Pan CT, Wang Q, Shi XH, Jonas JB, Wei WB. Optical coherent tomographic angiographic pattern of the deep choroidal layer and choriocapillaris after photodynamic therapy for central serous chorioretinopathy. Graefes Arch Clin Exp Ophthalmol 2019 Jul; 257(7): 1365–72.
33. Cennamo G, Montorio D, Comune C, et al. Study of vessel density by optical coherence tomography angiography in patients with central serous chorioretinopathy after low-fluence photodynamic therapy. Photodiagnosis Photodyn Ther 2020 Jun; 30: 101742.
34. Alovisi C, Piccolino FC, Nassisi M, Eandi CM. Choroidal Structure after Half-Dose Photodynamic Therapy in Chronic Central Serous Chorioretinopathy. J Clin Med 2020 Aug 24; 9(9): 2734.
35. Costanzo E, Cohen SY, Miere A, et al. Optical Coherence Tomography Angiography in Central Serous Chorioretinopathy. J Ophthalmol 2015; 2015: 134783.
36. Savastano MC, Lumbroso B, Rispoli M. In vivo characterization of retinal vascularization morphology using optical coherence tomography angiography. Retina 2015 Nov; 35(11): 2196–203.
37. Regatieri CV, Novais EA, Branchini L, et al. Choroidal thickness in older patients with central serous chorioretinopathy. Int J Retina Vitreous 2016 Sep 15; 2: 22.

38. Agrawal R, Seen S, Vaishnavi S, et al. Choroidal Vascularity Index Using Swept-Source and Spectral-Domain Optical Coherence Tomography: A Comparative Study. Ophthalmic Surg Lasers Imaging Retina 2019 Feb 1; 50(2): e26–e32.

39. Christou EE, Stavrakas P, Kozobolis V, Katsanos A, Georgalas I, Stefaniotou M. Evaluation of the choriocapillaris after photodynamic therapy for chronic central serous chorioretinopathy. A review of optical coherence tomography angiography (OCT-A) studies. Graefes Arch Clin Exp Ophthalmol 2022 Jun; 260(6): 1823–35.

Are Digital Methods Sufficiently Successful in Colour Determination for Monolithic All-Ceramic Crowns?

Lenka Vavřičková*, Martin Kapitán, Eliška Charlotte Wurfel

ABSTRACT

Objective: The aim of this study was to compare the visual assessment of tooth shade with the measurement using intraoral scanner (IOS) and spectrophotometer devices.

Methodology: The colour for a single unit implant supported crown was measured visually, using IOS, and spectrophotometer. The results of the digital methods were compared with the visual measurement.

Results: A complete colour match with the visual measurement was in 42.9% of cases for IOS, and in 33.3% of cases for spectrophotometry. The match in the colour value, hue, and chroma were in 61.9%, 95.2%, and 66.7% of cases, respectively, for the IOS; and in 61.9%, 61.9%, and 66.7% of cases, respectively, for the spectrophotometry. The differences between the IOS and spectrophotometry were not statistically significant.

Conclusions: The most reliable method for tooth colour selection is the visual measurement by an experienced dentist. IOS and spectrophotometer can be used as an alternative method, however in both cases they should be verified using visual measurement.

KEYWORDS

colour match; intraoral scanner; spectrophotometer; visual match

AUTHOR AFFILIATIONS

Department of Dentistry, Charles University, Faculty of Medicine in Hradec Králové, and University Hospital Hradec Králové, Czech Republic

* Corresponding author: Department of Dentistry, Sokolská 581, 500 05, Hradec Králové, Czech Republic; e-mail: vavrickoval@lfhk.cuni.cz

Received: 7 March 2022
Accepted: 8 December 2022
Published online: 2 February 2023

Acta Medica (Hradec Králové) 2022; 65(3): 99–104
https://doi.org/10.14712/18059694.2022.25

INTRODUCTION

The colour of prosthodontic restoration and beautiful smile design are some of the most important factors for modern dentistry from the patient's point of view. A perfect colour match between restorations is essential to patients (1). There are many ways how to find an optimal colour match between the natural teeth and a planned fixed restoration (2). Subjective color matching provided by dentists and dental technicians had the priority in the past but still is the most frequently applied method in dentistry (3). In present time we have a selection of devices which have been developed to provide a successful color selection (4).

Human optical system is able to recognize the light wavelength from 380 nm (violet) to 780 nm (red). The cones containing photosensitive pigments are responsible for the colour vision. They are sensitive to 3 basic colours: blue (448 nm), green (528 nm), and red (567 nm). Pigments are stimulated by light, then disintegrate and create an electrical impulse which is relayed to nerves. In total there are about 6–7 million cones placed in fovea centralis. Some studies describe gender dependent sensitivity of cones (5).

Choosing tooth colour shade can be influenced by several factors, such as physical, physiological, dental, and psychological. The physical factors include, for example, metamerism and the influence of background (2). Metamerism is described as the situation when two objects are noticed different when one factor out of three (source-object-receptor = human) varies, but the other two are constant (6). Object metamerism is describing the fact that colour of the same objects varies when the light source is changed (7). Receptor metamerism depends on sensitivity of cones. The influence of background is significant, because all teeth look lighter with darker background even if the colour is the same. One of the physiological factors is age related decrease of retinal ganglion cells. Dental factors are based on facts that various teeth have naturally different colour shades, particularly, their values (canine versus central incisor) (8, 9), and older people have naturally a richer colour shade with lower hues in cervical areas (8). There are no significant differences in tooth colour between males and females (10). Psychological factors describe the sensory adaptation. Sensory adaptation has an effect on decreasing sensitivity of receptor when the stimulus is repeating. Chromatic analytical interval indicates the time for choosing the colour without doubts and is about 5 s.

Light source can influence colour match as was mentioned earlier during the discussion of metamerisms. The light quality is determined by the colour temperature which is ideally 5500 K for the colour match.

The colour of an object consists of three dimensions: value, hue, and chroma. Value is the light quantity, that the object reflects in comparison with a bright white diffuser or a black absorber. The light object reflects the most of light, it means, it has the high value. Reversely the dark object absorbs the most of light and seems to be with low value. Hue is the light wavelength. It is depended on the wavelength of the light spectrum that is reflected/transmitted by the object. An opaque object does not transmit the light, rather it creates a so-called spectral reflection curve. A transparent object (e.g., glass) transmits light and creates a so-called spectral transmission curve. Teeth are translucent objects, they reflect and transmit light at the same time. Chroma is the result of the rates of energies of various monochromatic lights represented in the certain colour or concentration of the certain hue. Rich colours do not contain a white part (e.g., spectral colors). Rich colour is created by few lights (ideally only one) – the curve is narrow and colour can be easily recognized. Non-rich colours contain a white part (it is in principle a white colour with a "touch" of colours) (11).

The most used shade guide today for choosing the colour of teeth is Vitapan 3D Master® Shade Guide (Vita, Germany). The artificial teeth are classified according to the value – groups n. 1–5 (means all teeth in the same groups have got the same value). Except for groups 1 and 5, each group consists of 3 subgroups M, L, and R according to the various hues. L means light-yellow hue, M means medium-yellow-orange hue and R means red hue. Each subgroup contains 2 (for L and R – 1.5 and 2.5) or 3 (for M – 1, 2, 3) levels of chroma (12). VITA Classical A1-D4®-shade guide is older generally and universally used guide. Shade-hue is marked by letters; A-orange-red, B-yellow, C-grey, and D-brown. There are 4 numbers matching various value and chroma in each hue, where 1 means high value and low chroma and 4 means low value and high chroma (12).

Some limitations can occur using shade guides. They are especially related to the level of opalescence and translucency. To minimize all factors influencing the visual tooth shade choosing, it is recommended to follow some regulations. Some of them are as follows: suitable light source (5500 K), suitable background (light grey), avoiding rich colours near the object (lipstick, make-up, clothing), wet tooth surface (enamel dehydration), eye to eye position (same body height or proper patient positioning), distance 30–50 cm, choosing in the morning (eye fatigue) and preferably the colour selection together with the dental technician. It is also useful to take photos of the teeth, a colour one and a grayscale one.

There are some devices helpful for this difficult task. A dental spectrophotometer measures the spectral reflectance or transmittance curve of the tooth. Light is released from light source in the spectrophotometer and then dispersed by a prism into a spectrum of different wavelengths between 380–780 nm. The spectrophotometer then measures the amount of the light reflected from the specimen for each wavelength and converts the data into numerical values of colour. Before measurement automatic calibration is needed. Intraoral scanners are based on non-contact optical acquisition technologies used by different IOS cameras to produce precise 3-dimensional renderings of soft and hard tissue. There are many principles for IOS systems – confocal microscopy with ultrafast optical scanning or laser light beams based on parallel confocal principles etc. Automatic shade matching is incorporated into the software. This technology collects actual shade values from several views, considering all angles captured by the scanner (13).

MATERIAL AND METHODS

The study was approved by the Ethics committee of the University Hospital Hradec Králové (ref. No. 201903S08P). Participation in the study was voluntary, each participant signed an informed consent. In total, 23 patients were asked for study cooperation.

The colour match for fixed single implant supported crowns during the regular treatment procedure in University Hospital Hradec Králové from October 2021 to January 2022 was determined.

The colour was selected in three different ways; the first was using Vitapan 3D Master® Shade Guide (VITA Zahnfabrik, Bad Sackingen, Germany) for visual measurement (Figure 1), second was with an IOS system (3Shape TRIOS Move +, 3Shape, Denmark) during intraoral scanning (Figure 2), and third was using spectrophotometer (Figure 3) (VITA Easyshade© Compact Advance, VITA Zahnfabrik, Bad Sackingen, Germany).

One evaluator analyzed the colour using Vitapan 3D Master® Shade Guide under given conditions: daylight in the morning with standard light source of the room, light grey background, wet tooth surface of referential tooth, and eye to eye position with distance 50 cm.

The result of the visual measurement was considered as the final colour for the crown fabrication. The material used for the restoration was monolithic zirconia oxide dental ceramic. The colour was selected according to a natural tooth in the same segment of the same jaw without any filling or restorations, not even next to gap. The selections were done in sitting patients following all recommendations for producers (the probe tip of spectrophotometer placed as flat as possible on the tooth surface) or general rules for visual match with the same light source as mentioned above. Measurement was done on the middle section of the vestibular surface of the referential tooth while it was wet. Light grey background with eye to eye position in distance 30–50 cm was used. The visual match was done during the morning hours.

Vitapan 3D Master® Shade Guide was used for primary statistical analysis, where the total colour and separate parameters of colour (value, hue, and chroma) were compared. During the secondary analysis, VITA LinearGuide 3D-Master® was used as linear colour scale for an assesment of the deviation magnitudes. The deviation to the lighter colour was denoted as negative value, whereas the darker colour was indicated with positive value.

The gathered data were analyzed in MS Excel using the methods of descriptive statistics, chi-square test, Fisher's exact test, Wilcoxon test, and One-sample proportion test. The level of statistical significance was set at $\alpha = 0.05$.

RESULTS

A total of 21 patients (11 men, 10 women) participated in the study, two of the patients rejected the study participation because of the lack of time. The study participation was 91.3% of possible patients. Fixed single implant-supported crown was planned for all of the participants. In 20 patients, the crown was in a lateral section of a jaw, one crown was in a frontal section. 12 crowns were localised in the upper jaw, nine of them in the lower jaw. Table 1 shows the localisations of the crowns, the natural teeth used for the colour measurement and the colours selected by the three compared methods.

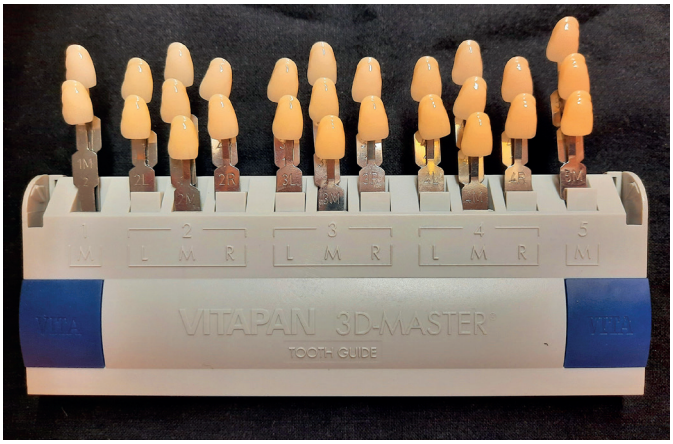

Fig. 1 Vitapan 3D Master® Shade Guide (Vita, Germany).

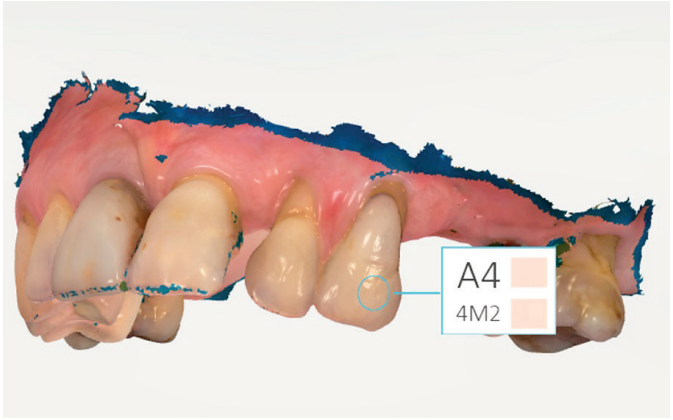

Fig. 2 Selected colour on referential tooth with IOS system 3Shape TRIOS Move + (3Shape, Denmark).

Fig. 3 Spectrophotometer VITA Easyshade© Compact Advance (VITA, Germany).

Tab. 1 Localisation of single unit crown, natural tooth matching and colours chosen with different methods.

Single implant-supported crown	Natural tooth matching	IOS	Spectrophotometer	Human eye-resulting colour used
46	47	2M2	2M2	3M2
46	44	2M3	3L2.5	4L1.5
24	34	4M2	3M3	4M2
14	15	4M3	2R2.5	4M2
36	35	3M1	3M2	3M2
36	35	3M3	3M3	3M3
46	45	4M2	3M3	3M2
46	45	4M2	3L1.5	3M2
26	25	3M1	3M2	3M2
36	35	3M3	3M3	3M3
24	34	3M2	3M3	3M2
25	24	2M2	2M2	2M2
46	44	3M2	3M3	3M2
26	21	2M1	1M2	3M2
22	21	3M2	3M2	3M2
26	25	2M2	2M2	2M2
16	11	2M2	2M1	3M2
45	44	2M2	2M2	3M2
14	42	3M1	2L1.5	2M2
36	34	2M3	2M3	2M2
46	44	3M2	1M1	3M2

Figure 4 shows the correspondence of the colours selected by IOS and spectrophotometer with the visual measurement in the overall colour and in all parameters of colour separately. The differences between IOS and spectrophotometer were not statistically significant (Fisher's exact test-p = 0.1588, p = 0.1637, p = 0.381, p = 1 for total colour, value, hue, and chroma, respectively.

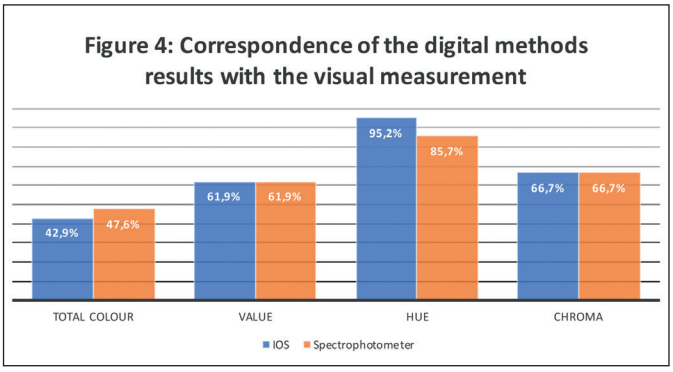

Fig. 4 Correspondence of the digital methods results with the visual measurement.

Figure 5 shows the grades of the colour deviation of both digital methods from the visual measurement. The median value and quartiles were 0 (–5, 1.5) and 0 (–7, 0) for IOS and spectrophotometer, respectively. The differences between both digital methods from the visual measurement were not statistically significant (Wilcoxon test, IOS: p = 0.433 and spectrophotometer: p = 0.0505).

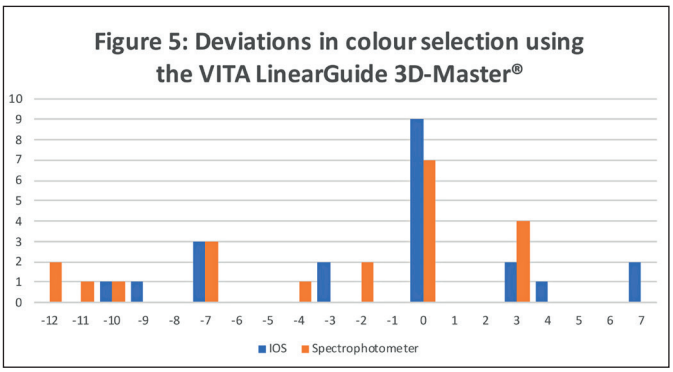

Fig. 5 Deviations in colour selection using the VITA LinearGuide 3D-Master®.

For IOS the negative deviation was found in 33.3% of cases (n = 7), no deviation in 42.9% (n = 9), and positive deviation in 23.8% (n = 5). For spectrophotometer the negative deviation was found in 47.6% of cases (n = 10), no deviation in 33.3% (n = 7), and positive deviation in 19.1% (n = 4).

The trend to positive or negative colour deviation was not statistically significant for both methods (one-sample proportion test, IOS: p = 0.7744 and spectrophotometer: p = 0.18).

DISCUSSION

The colour selection for new fabricated restorations is one of the most important tasks for dentists. Although the

VITA Classical®shade guide is generally and universally used, the Vitapan 3D Master® Shade Guide was used for this study. The reason for this decision was that several recent studies considered VITA Classical A1-D4®shade guide the least consistent with the examined tooth (14). The Vitapan 3D Master® Shade Guide achieved more consistent results in repetitive shade selection (15). VITA Linearguide 3D-Master has arrangement similar to the VITA Classical A1-D4®shade guide but using all colour aspects as Vitapan 3D Master® Shade Guide and is more synoptical for beginners. Some studies revealed significant advantage for colour match using VITA Linearguide 3D-Master compared to Vitapan 3D Master® Shade Guide (16). To maximize shadow matching it is also recommended to use digital photography, however, the results were worse compared to the visual measurement and IOS color match (12).

IOS digital systems have benefited from their speed and ability to facilitate communications with patients as well as dentists and dental technicians (17), but to fulfill the rule of chromatic analytical interval, the visual match timing is similar to digital systems. Previous studies have found that the examiner's experience may have greatly impacted the tooth colour determination (5). Moreover, visual tooth shade determination can be learned (18). These facts may result in a higher success rate of the visual match compared to the digital methods. Thus, a not-experienced young dentist can be more familiar with digital devices. Gender can also play a role in consideration of the differences between the methods. Men are likely to rely more on the digital methods, as they suffer from colour perception deficiencies more frequently (8%) than women (0.5%) (5).

Some clinical studies declare that the instrumental methods for colour shade matching were more reliable than the visual methods (19). Studies also have shown different results of spectrophotometers and IOS systems (20). IOS systems are a good alternative for tooth shade selection (17). The colour match with IOS was superior to visual colour match but using A1–D4 values (21).

The spectrophotometer reported higher accuracy, reliability and repeatability in shade selection followed by photocolorimetric method. Knowledge and practice in the shade selection protocol are necessary for proper shade matching (15). The colour determination with IOS was more repeatable than when using visual systems (22). In this study, both digital methods are considered as an alternative method, especially for value and chroma. They showed a high correspondence in hue, but the value and chroma should be always verified by the visual measurement. That result is in accordance with another study confirming the fact, that the best matching shade was selected using the visual method. IOS can be used as an alternative method of shade selection, but it is recommended to verify the measurements using the visual method (14).

Different factors can affect the accuracy and precision of the tooth shade selection methods and devices (23). The light source as well as having a neutral background in visual methods are most important. For IOS, the most important factor is the way of reading the information about the colour match. IOS can measure the attributes of colour in very small areas, so for one particular tooth we can have many different colour matches. A small area means the average colour for every 3–5 mm on the tooth surface so the device provides a so called "colour map" (24). All-ceramic crowns fabricated as monolithic are preferred for lateral segment, which needs to simplify that information into one shade. That is the reason why it is more difficult to find proper colour. In case of veneered all-ceramic crowns, where the colour map can be respected by dental technician, this single colour is not necessary. It can cause that, the colour match was not perfect with IOS device. Spectrophotometer results could be influenced by difficult positioning of the device tip to a flat surface. Vestibular surface of the teeth is always convex.

The colour match can be also influenced by different crown material especially for monolithic crowns. Some hybrid ceramic has better color match for frontal teeth (VITA Enamic Translucent), other ones for lateral teeth (VITA Enamic HT) (25).

The limitation of this study was quite small number of the participating patients. Further research is needed to confirm the results using higher number of participants. Visual measurement of colour shade for prosthodontic restorations is the widespread method used by dental practitioners. The colour determination by only one experienced prosthodontist for visual measurement is an advantage, less experienced dentist can have different results.

CONCLUSION

The colour determination for implant-supported crowns can be realized by all methods used in this study. The congruence of both digital methods with the visual assesment was relatively low, even though the differences were not statistically significant. IOS and spetrophotometer can be used as an initial method, but the colour assesment should be verified visually according to authors´ recommendation and literature search.

DISCLOSURE

The authors declare no conflicts of interest related with this article. The authors are not in any relationships with the producers of the devices and materials used in this study.

ACKNOWLEDGEMENTS

The authors would like to thank RNDr. Eva Čermáková (Computer Technology Center, Charles University, Faculty of Medicine in Hradec Králové, Czech Republic) for statistical analysis and all participants for patience during the colour selection.

The study was supported by the Charles University's COOPERATIO Program, Research Area DENTAL MEDICINE.

REFERENCES

1. Baldwin DC. Appearance and esthetics in oral health. Community Dent Oral Epidemiol 1980; 8: 224–56.
2. Corcodel N, Helling S, Rammelsberg P, Hassel AJ. Metameric effect between natural teeth and shade tabs of a shade guide. Eur J Oral Sci 2010; 118: 311–6.

3. Van der Burgt TP, Ten Bosch JJ, BorsboomPCF, Kortsmit WJPM. A comparison of new and conventional method for quantification of tooth color. J Prosthet Dent 1990; 63: 155–62.
4. Dozic A, Kleverlaan CJ, El-Zohairy A, Feilzer AJ, Khashayar G. Performance of five commercially available tooth color-measuring devices. J Prosthodont 2007; 16: 93–100.
5. Haddad HJ, Jakstat HA, Arnetzl G, et al. Does gender and expirience influenceshade matching quality? J Dent 2009; 37: e40–44.
6. Fondriest J. Shade matching in restorative dentistry: the science and strategies. Int J Periodontics Restorative Dent 2003; 23: 467–79.
7. Yu B, Lee YK. Colour difference of all-ceramic materials by the change of illuminants. Am J Dent 2009; 22: 73–8.
8. Goodkind RJ, Keenan K, Schwabacher WB. Use of fiberoptic colorimeter for an in vivo color measurement of 2830 anterior teeth. J Prosthet Dent 1987; 58: 535-542.
9. Zhao Y, Zhu J. In vivo color measurement of 410 maxillary anterior teeth. Chin J Dent Res 1998; 3: 49–51.
10. Jahangiri L, Reinhardt SB, Mehra RV, Matheson PB. Relationship between tooth shade value and skin colour: an observational study. J Prosthet Dent 2002; 87: 149–52.
11. Joiner A. Tooth color: a review of the literature. J Dent 2004; 32: 3–12.
12. McLaren EA, Schoenbaum T. Combine conventional and digital methods to maximize shade matching. Inside Dental Assisting 2012; 8: 2.
13. Jurim B, Jurim A. A review of intraoralscanning technology. Inside Dental Technology 2019; 10: 9.
14. Czigola A, Roth I, Vitai V, Feher D, Hermann P, Borbely J. Comparing the effectiveness of shade measurement by intraoral scanner, digital spectrophotometer, and visual shade assesment. J Esthet Restor Dent 2021; 33: 1166–74.
15. Borse S, Chavare SH. Tooth shade analysis and selection in prosthodontic. J Indian Prosthodont Soc 2020; 20: 131–40.
16. Paravina RD. Performance assesment of dental shade guides. J Dent 2009; 37: e15–20.
17. Brandt J, Nelson S, Lauer HC, von Hehn U, Brandt S. In vivo studyfor tooth colour determination-visual versus digital. Clin Oral Investig 2017; 21: 2863–71.
18. Blum SL, Horn M, Olms C. A comparison of intraoral spectrophotometers-Are there user specific differences? J Esthet Restor Dent 2018; 30: 442–8.
19. Liberato WF, Barreto IC, Costa PP, Costa de Ameida C, Pimentel W, Tiossi R. A comparison between v sual, itraoral scanner, and spectrophotometer shade matching: A clinical study. J Prosthet Dent 2019; 121: 271–5.
20. Yilmaz B, Irmak O. Outcomes of visual tooth shade selection performed by operators with different expirience. J Esthet Restor Dent 2019; 31: 500–7.
21. Rutkunas V, Dirse J, Bilius V. Accuracy of an intraoral digital scanner in tooth color determination. J Prosthet Dent 2020; 123: 322–9.
22. Reyes J, Acosta P, Ventura D. Repeatability of the human eye compared to an intraoral scanner in dental shade matching. Helion 2019; 5: e02100.
23. Tabatabaian F, Beyabanaki E, Alirezaei P, Epakchi S. Visual and digital tooth shade selection methods, related effective factors and conditions, and their accuracy and precision: A literature review. J Esthet Restor Dent 2021; 33: 1084–104.
24. Chu SJ, Trushkowsky RD, Paravina RD. Dental color matching instruments and systems. Review of clinical and research aspects. J Dent 2010; 2, e2–16.
25. Pop-ciutrila IS, Dudea D, Eugenia Badea M, Moldovan M, Cimpean SI, Ghinea R. Shade correspondence, color, and translucency differences between human dentine and CAD/CAM hybrid ceramic system. J Esthet Restor Dent 2016; 28: 46–55.

The Role of FXR-Signaling Variability in the Development and Course of Non-Alcoholic Fatty Liver Disease in Children

Yuriy Stepanov, Natalia Zavhorodnia*, Inna Klenina, Olena Hrabovska, Viktoria Yagmur

ABSTRACT

Introduction: Genetic mechanisms among many other factors play a crucial role in the development and progression of nonalcoholic fatty liver disease (NAFLD). The farnesoid X-receptor (FXR) regulates the expression of target genes involved in metabolic and energy homeostasis, so it can be assumed that genetic variations within the *NR1H4* gene, encoding FXR, can affect the development or progression of associated diseases, including NAFLD.

The aim: To study the association of SNP rs11110390 *NR1H4* gene with the probability of development and course of NAFLD in children.

Materials and methods: 76 children aged 9–17 years and overweight were examined. According to controlled attenuated parameter (CAP) measurement (Fibroscan®502touch) children were divided into 2 groups: group 1 consisted of 40 patients with NAFLD, group 2 was composed by 36 patients without hepatic steatosis. According to genetic testing children were divided into 3 subgroups – children with CC-, CT-, TT-genotype SNP rs11110390 *NR1H4* gene.

Results: The frequency of TT-genotype SNP rs11110390 *NR1H4* gene detection in children with NAFLD was 17.5% versus 2.8% in the control group ($p < 0.05$). In children with TT-genotype SNP rs11110390 *NR1H4* gene the liver stiffness ($p < 0.05$) and CAP ($p = 0.1$) were higher than in patients with CC- and CT-genotypes. Patients with the TT-genotype differed from CC-genotype patients with lower levels of IL-10 ($p < 0.05$) and pro-inflammatory cytokine balance ($p < 0.05$). An increase in the concentration of taurine-conjugated bile acid fractions in the hepatic and gallbladder's bile in children with TT-genotype SNP rs11110390 *NR1H4* ($p < 0.05$) was demonstrated.

Conclusions: SNP rs11110390 *NR1H4* is associated with an increased probability of NAFLD development in children. An increase in the steatosis degree and liver stiffness in combination with increased taurine-conjugated bile acids fractions in the hepatic and gallbladder's bile, shift in cytokine balance due to a decrease in IL-10 level in children with TT-genotype SNP rs11110390 *NR1H4* were observed.

KEYWORDS

farnesoid X-receptor; single nucleotide polymorphism; nonalcoholic fatty liver disease; children

AUTHOR AFFILIATIONS

SI "Institute Gastroenterology of the National Academy of Medical Sciences of Ukraine", Dnipro, Ukraine

* Corresponding author: Pediatric Gastroenterology Department, SI "Institute Gastroenterology of the National Academy of Medical Sciences of Ukraine", Dnipro, Ukraine; e-mail: nzavgorodni75@gmail.com

Received: 19 July 2021
Accepted: 11 December 2022
Published online: 2 February 2023

Acta Medica (Hradec Králové) 2022; 65(3): 105–111
https://doi.org/10.14712/18059694.2022.26

INTRODUCTION

The rapid increase in the prevalence of nonalcoholic fatty liver disease (NAFLD) in recent decades is the result of a combined influence of environment, endogenous factors (such as eating behavior, physical activity, intestinal microbiota composition), and genetic predisposition (1). Among many others genetic mechanisms play an important role in the development and progression of NAFLD (2). The significance of genetic variability underlying the susceptibility to NAFLD has been confirmed in numerous modern genome-wide association studies (3). Studies of candidate genes demonstrated the influence of certain genetic variants on lipid metabolism, inflammation, insulin signaling, fibrogenesis, and oxidative stress activity which determine the severity of NAFLD (4–6). Nowadays, the concept of the role of individual genes/proteins in NAFLD is gradually being replaced by the study of multiple causal interactions using systemic biology approaches. The "NAFLD-Reactome" project confirmed the role of nuclear receptors in the related gene expression regulation in the pathogenesis of NAFLD (7). The *NR1H4* gene encoding farnesoid-X-receptor (FXR) is a member of the nuclear receptors superfamily, so-called ligand-activated transcription factors. It regulates a significant number of target genes involved in a wide range of metabolic processes, such as lipid, carbohydrate, and energy metabolism, bile acid homeostasis, inflammation, cell proliferation, differentiation and death, and regulation of the intestinal microbiota composition and activity (8, 9). Although FXR is most widely presented in tissues involved in the bile acids circulation, including the liver, intestine, and bile duct epithelium, FXR expression is also found in renal tubular cells, adrenal glands, pancreatic tissue, adipocytes, cardiomyocytes, myocytes, endothelial and immune cells (10). The effects of FXR activation are tissue-specific. Both hepatic (hFXR) and intestinal (iFXR) receptors are important mediators of reverse inhibition of bile acid synthesis and induction of bile acids transporters expression, protecting hepatocytes and enterocytes from excessive bile acids toxicity. iFXR activation mainly leads to inhibition of bile acid synthesis, while hFXR activation – to changes in the bile acids pool composition (11). In general, the small number of non-synonymous single nucleotide polymorphisms (SNPs) in the *NR1H4* gene compared to other genes indicates its evolutionary stability and confirms its crucial importance for cell homeostasis and function (12). Considering that FXR is a key metabolic regulator, it is likely that genetic variation within the *NR1H4* gene may have an influence on the development or progression of metabolic-associated diseases (13). Unfortunately, to date, the contribution of *NR1H4* polymorphisms to the NAFLD formation probability and clinical consequences for NAFLD remains unclear.

THE AIM

To study the association of SNP rs11110390 *NR1H4* gene with the probability of development and course of NAFLD in children.

MATERIALS AND METHODS

The study included 76 overweight and obese caucasian children aged 9 to 17 years (average age 12.3 ± 2.5 years). The presence of hepatic steatosis was determined by transient elastometry (FibroScan®502touch, Echosens, France) with the measurement of the controlled attenuation parameter (CAP). According to the presence of NAFLD, children were divided into 2 groups: group 1 (main) consisted of 40 patients with NAFLD, group 2 (control) consisted of 36 patients without hepatic steatosis. To study the association of SNP with laboratory-instrumental data, an intragroup analysis was performed: according to the molecular genetic testing the children with NAFLD were divided into 3 subgroups: children with CC-, CT-, TT-genotypes SNP rs11110390 *NR1H4* gene. The groups did not have significant differences in age and gender. The study has been performed according to the Declaration of Helsinki. The informed consent has been obtained from all patients. All procedures have been approved by the local ethics committee (certificate number 4).

Genetic study to determine the presence of polymorphic variants of the *NR1H4* gene (SNP rs11110390) was conducted in the Scientific Institution of Genetic and Immune Pathology and Pharmacogenetics of "Ukrainian Medical Stomatological Academy". DNA isolation was performed using a set of reagents "DNA-EXTRAN-1" (LLC "NPF SINTOL", Russia) from samples of fasting blood. Determination of the polymorphic variant of the *NR1H4* gene (rs11110390) was performed by allele-specific polymerase chain reaction (PCR) using fluorogenic samples to detect specific products in 25 μl of the reaction mixture, which included: 12.5 μl of 2 × TagMan Master Mix amplification solution; 1.25 μl of TagMan SNP Genotyping Assays containing specific nucleotide sequences for allele C and allele T; and DNA solution in nuclease-free water for PCR (Thermo Fisher Scientific, USA). Polymorphic alleles of the *NR1H4* gene (rs11110390) were amplified and detected in real time by measuring the fluorescent signal from the amplification products in each cycle, the intensity of which was proportional to the concentration of the final PCR product. Amplification was performed under the following conditions: the first cycle took place at a temperature of 95 °C for 10 minutes. The amplicons were accumulated in the next 40 cycles according to the following temperature parameters: 95 °C for 15 seconds, 60 °C for 60 seconds.

Quantitative determination of the concentration of IL-6, IL-10, TNF-α in the serum was performed with enzyme-linked immunosorbent assay (Vector-Best, Russia) using an analyzer "Stat Fax 303 Plus" (USA).

The content of total cholesterol (TC), triglycerides (TG), high-density lipoprotein (HDL) in the serum was determined using reagent kits "Cormey" (Poland) using a biochemical analyzer Stat Fax 1904 Plus, Awareness Technology (USA). Low-density lipoprotein (LDL) was calculated by Friedwald's formula. Very low density lipoprotein (VLDL) was determined by empirical calculations of TG levels.

Bile from patients was obtained by duodenal sounding. As a stimulator of bile secretion was used a solution with 33% $MgSO_4$. Determination of the content of taurocholic (TC), taurodeoxycholic (TDC), glycocholic (GC) and

Tab. 1 Distribution of alleles and genotypes of SNP rs11110390 *NR1H4* in the studied groups.

SNP ID	Allele frequency							Genotype frequency						
	Groups	Total		NAFLD		Control		Groups	Total		NAFLD		Control	
	Allele	n	%	n	%	n	%	Genotype	n	%	n	%	n	%
rs11110390	C	97	63.8	47	58.8	50	69.4	CC	29	38.2	14	35.0	15	41.7
								CT	39	51.3	19	47.5	20	55.6
	T	55	36.2	33	41.2*	22	30.6	TT	8	10.5	7	17.5*	1	2.8
Total		152	100	80	100	72	100		76	100	40	100	36	100

Note: * $p < 0.05$ – significance of differences by Fisher's criterion versus the control group.

glycodeoxycholic (GDC) bile acids in bile was performed using the method of thin-layer chromatography (14). The content of bile acids and cholesterol was determined using a densitometer BIAN-170 (λ = 620 nm) after staining the samples on the calibration curves.

Statistical processing of the results was performed using the application package Statistica 6.1 (serial number AGAR909 E415822FA). The conformity of the data distribution to the normal distribution was checked using the Shapiro – Wilk method. The mean (M) and standard deviation (SD) or median (Me), lower (Q1) and upper (Q2) quartiles were used to describe the data. For comparison ANOVA + post hoc test has been applied. Fisher's test was used to compare qualitative features belonging to nominal or ordinal scales. Statistical significance was assessed at a level not lower than 95.0% ($p < 0.05$).

RESULTS

According to the results of molecular genetic examination, the SNP rs11110390 of the *NR1H4* gene in the heterozygous state (CT) was detected in 51.3% of all examined children, while the homozygous (TT) condition was present in 10.5% children (Table 1).

CC-genotype of the *NR1H4* gene was observed in 35% of NAFLD children, CT-genotype – in 47.5% of NAFLD children, and TT-genotype – in 17.5% (Table 1). The frequency of TT-genotype *NR1H4* gene detection in children with NAFLD significantly differed from the control group (17.5% vs 2.8%, $p < 0.05$). The frequency of the minor (T) allele detection among NAFLD children was 41.2% that was significantly higher than in the control group (30.6%) (Table 1).

ASSOCIATION OF SNP RS11110390 *NR1H4* WITH ANTHROPOMETRIC PARAMETERS

The body mass index (BMI) and waist circumference mean values in CT- and TT-genotypes SNP rs11110390 *NR1H4* gene carriers were increased, but the differences were not significant ($p > 0.05$) (Table 2).

ASSOCIATION OF SNP RS11110390 *NR1H4* GENE WITH BIOCHEMICAL PARAMETERS

When comparing the hepatic transaminases activity, no significant differences were found between subgroups (Table 3), but the average levels of γ-glutamyltranspeptidase (GGT) were significantly higher in TT-genotype SNP rs11110390 *NR1H4* carriers (Fig. 1).

Tab. 2 Comparison of the anthropometric parameters depending on the SNP rs11110390 *NR1H4* genotype.

Anthropometric parameters	SNP rs11110390 genotype			p
	CC	CT	TT	
	M ± SD	M ± SD	M ± SD	
BMI, kg/m²	23.8 ± 3.9	24.9 ± 4.3	26.3 ± 3.3	0.2
Waist circumference, cm	81.3 ± 3.2	82.7 ± 2.8	84.7 ± 1.9	0.4

Note: p – significance of differences according to F-criterion between the TT-genotype and CC-genotype patients.

Tab. 3 Comparison of the biochemical parameters depending on the SNP rs11110390 *NR1H4* genotype.

Biochemical parameters	SNP rs11110390 genotype			p
	CC	CT	TT	
	M ± SD	M ± SD	M ± SD	
ALT, U/l	37.2 ± 1.6	36.8 ± 1.4	40.3 ± 1.2	>0.05
AST, U/l	28.7 ± 1.2	29.8 ± 1.1	32.3 ± 0.9	>0.05
GGT, U/l	18.6 ± 0.9	19.2 ± 0.8	27.7 ± 1.1	<0.05

Note: p – significance of differences according to F-criterion between the TT-genotype and CC-genotype patients.

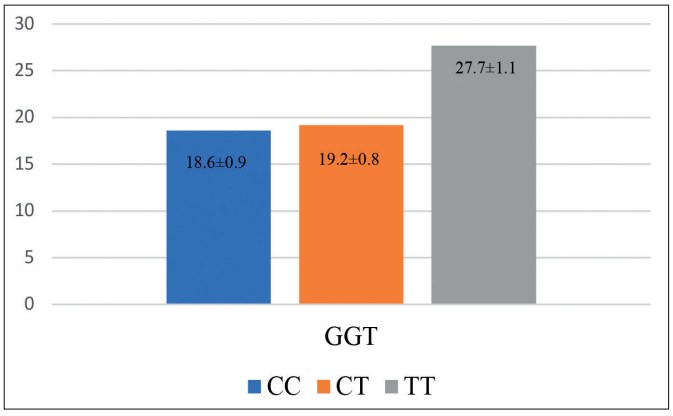

Fig. 1 Mean GGT values depending on the SNP rs11110390 *NR1H4* genotype.

ASSOCIATION OF SNP RS11110390 *NR1H4* GENE WITH LIVER STRUCTURE CHANGES

Children with TT-genotype of SNP rs11110390 *NR1H4* gene were characterized by significantly higher liver stiffness mean values compared to patients with CC- and CT-genotypes ($p < 0.05$) (Fig. 2A). Patients with the TT-genotype also differed from CT- and CC-genotypes carriers with higher CAP levels, but the differences between the groups were a trend ($p = 0.1$) (Fig. 2B).

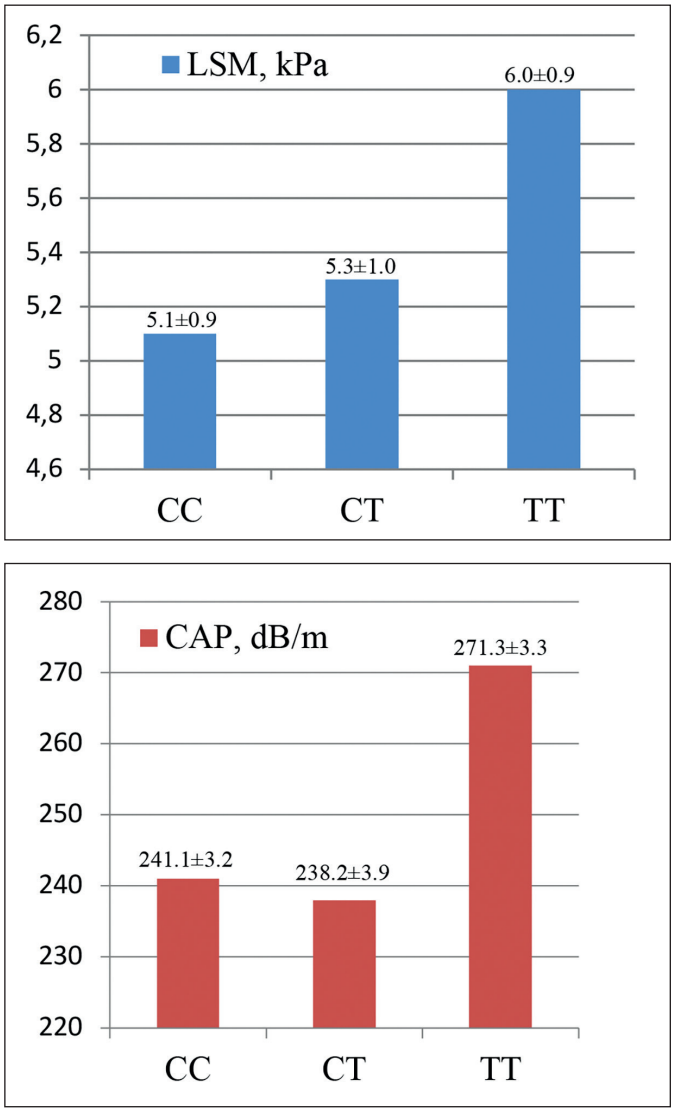

Fig. 2 Liver stiffness (A) and CAP (B) depending on the SNP rs11110390 *NR1H4* genotype.

ASSOCIATION OF SNP RS11110390 *NR1H4* GENE WITH THE CYTOKINE PROFILE

Patients with CT-genotype in contrast to patients with CC-genotype of SNP rs11110390 *NR1H4* gene were characterized by increased levels of proinflammatory cytokines TNF-α and IL-6, but the balance of cytokines was maintained due to a unidirectional increase in the concentration of anti-inflammatory cytokine IL-10 (Table 4). Patients with TT-genotype SNP rs11110390 *NR1H4* differed from patients with CC-genotype with lower IL-10 levels ($p < 0.05$) and a shift in the balance of cytokines towards proinflammatory state (increase in TNF-α / IL-10, $p < 0.05$).

Tab. 4 Cytokine profile depending on the SNP rs11110390 *NR1H4* genotype.

Cytokines	SNP rs11110390 *NR1H4* genotype		
	CC	CT	TT
	Me (Q25, Q75)	Me (Q25, Q75)	Me (Q25, Q75)
IL-6, pg/ml	0.9 (0.4; 1.3)	2.3* (0.3; 5.5)	2.1* (0.2; 4.3)
TNFα, pg/ml	0.7 (0.4; 1.1)	2.1* (0.4; 3.8)	1.1 (0.2; 2.0)
IL-10, pg/ml	2.6 (1.1; 4.1)	4.7* (2.2; 7.3)	1.5* (0.1; 2.9)
TNFα/IL10	0.6 (0.1; 1.1)	0.6 (0.3; 0.8)	2.1* (0.7; 4.9)

Note: * $p < 0.05$ – the significance of differences according to the F-criterion compared to children with CC-genotype.

ASSOCIATION OF SNP RS11110390 *NR1H4* GENE WITH LIPID PROFILE PARAMETERS

The study of lipid metabolism depending on the presence of SNP rs11110390 *NR1H4* gene showed that in children with TT-genotype it was observed an increase of the atherogenicity index (AI) due to a shift in the balance of HDL / non-HDL to the HDL decrease, but the differences did not have sufficient significance (Table 5).

Tab. 5 Lipid spectrum parameters depending on the SNP rs11110390 *NR1H4* genotype.

Lipid parameters	SNP rs11110390 *NR1H4* genotype			p
	CC	CT	TT	
	M ± SD	M ± SD	M ± SD	
TG, mmol/l	1.2 ± 0.8	0.8 ± 0.4	0.8 ± 0.4	0.2
HDL, mmol/l	1.0 ± 0.4	1.0 ± 0.3	0.8 ± 0.2	0.4
Non-HDL, mmol/l	3.0 ± 0.3	2.5 ± 0.3	3.2 ± 0.2	0.9
VLDL, mmol/l	0.9 ± 0.3	0.4 ± 0.2	0.3 ± 0.2	0.1
AI	3.5 ± 1.4	3.7 ± 1.4	3.9 ± 0.9	0.2

Note: p – significance of differences according to the F-criterion between the parameters of the patients with TT- and CC-genotype.

ASSOCIATION OF SNP RS11110390 *NR1H4* GENE WITH THE BIOCHEMICAL BILE COMPOSITION PARAMETERS

Comparative analysis of the bile acid fractions concentration in patients depending on the SNP rs11110390 *NR1H4* genotype showed a significant increase in the concentration of TC and TDC in gallbladder's bile (bile B), as well as TC in hepatic bile (bile C) (Table 6).

Tab. 6 Biochemical bile composition depending on the SNP rs11110390 *NR1H4* genotype.

Parameters	SNP rs11110390 *NR1H4* genotype			p
	CC	CT	TT	
	M ± SD	M ± SD	M ± SD	
TC bile B, mmol/l	0.4 ± 0.1	0.9 ± 0.1	2.9 ± 0.1	< 0.05
TDC bile B, mmol/l	0.8 ± 0.2	1.4 ± 0.2	2.7 ± 0.3	< 0.05
TC bile C, mmol/l	0.1 ± 0.0	0.3 ± 0.0	0.5 ± 0.1	< 0.01

Note: p – significance of differences according to the F-criterion between the parameters of the patients with TT- and CC-genotype.

DISCUSSION

The SNP rs11110390 *NR1H4* gene that we have studied is intronic and localized in the noncoding region of the gene. According to our data, the frequency of the minor T-allele detection among children with NAFLD was 41.2%, that significantly exceeds such parameter of the obese children (36.2%), which coincides with the ALFA-project data that demonstrate the variability of the minor T-allele prevalence in different populations (Fig. 3) with a frequency in the European population of 32.4% (15).

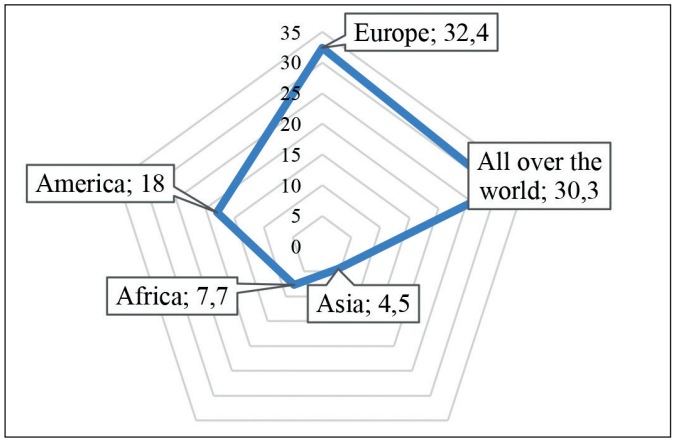

Fig. 3 Frequency of the minor T-allele detection of SNP rs11110390 *NR1H4* gene in different populations (15).

The prevalence of homozygous carriage of SNP rs11110390 *NR1H4* gene among children with NAFLD also differed significantly from the control group and was 17.5%, which may allow the possibility of the association of TT-genotype with NAFLD development. The prevalence of the minor allele and polymorphic genotypes varies considerably between different cohorts of patients. So, Nijmeijer et al. (2011) in the study of adult patients with Crohn's disease and ulcerative colitis demonstrated 32.2% prevalence of the minor T-allele of SNP rs11110390 *NR1H4* gene (16). Lutz et al. (2014), in turn, showed 8.9% prevalence of TT-genotype of SNP rs11110390 *NR1H4* gene among adults with complication by ascites cirrhosis (17).

According to the recent data the association of the wide spectrum of SNP of coding and non-coding regions in the *NR1H4* gene has been confirmed with various dysmetabolic and inflammatory diseases, such as obesity, gallstone disease, intrahepatic cholestasis of pregnancy, Crohn's disease, ulcerative colitis, spontaneous bacterial peritonitis etc. (16–26). Van Mil et al. (2009) identified 4 new SNPs *NR1H4* gene accompanied by functional translation insufficiency and decrease in protein activity in pregnant women with cholestasis, assuming its association with the intrahepatic cholestasis and other cholestatic diseases and dyslipidemia (26). However, a study in an extended cohort (563 pregnant women of European descent with cholestasis) did not confirm the association of these polymorphisms (mostly intronic) with susceptibility to the disease due to their low population frequencies (25). It should be noted that intronic mutations in general account for approximately 10% of all known human pathogenic mutations are accompanied by various rearrangements of mature mRNA due to the influence of SNP on the efficiency of splicing and alternative splicing (27). Introns make up about 24% of the human genome and they have the ability to regulate gene expression through the formation of non-functional or rapidly degrading RNA (negative regulation), intron-mediated enhancement of transcription activity, splicing rate control (28). Therefore, according to the function of introns in the regulation of gene expression, intronic mutations are often associated with severe pathological consequences.

In our study, significant differences in anthropometric parameters (BMI, waist circumference) between patients with different genotypes of SNP rs11110390 *NR1H4* gene were not found in contrast to van den Berg et al. (2009), who demonstrated a strong association between SNP *NR1H4* gene, BMI and waist circumference, assuming the effect of FXR on the adipose tissue distribution and its role in the development of obesity (18). Probably, the differences may be explained by the age difference of the cohorts of patients and the small proportion of morbidly obese patients in our study.

TT-genotype of SNP rs11110390 *NR1H4* gene, according to our data, was associated with impaired bile acid homeostasis: children with TT-genotype showed changes in the biochemical composition of hepatic and gallbladder bile due to increased concentrations of taurine-conjugated fractions associated with biochemical markers of cholestasis (GGT). This is explainable since the leading function of FXR and its target genes is the control of the synthesis, enterohepatic circulation and detoxification of bile acids (29). High level of FXR expression in the gastrointestinal tract allow FXR to play the role of a sensitive sensor of bile acids concentration in the liver and enterocytes, to mediate negative feedback to maintain constant levels of bile acids in hepatocytes and prevent liver damage and cholestasis, to control bile acids reabsorption into the portal bloodstream, to maintain the barrier function of the intestine. FXR-knockout animal models demonstrate the importance of FXR function in maintaining bile acid homeostasis (30).

Disruption of FXR signaling in an experimental model of steatosis in mice on a high-fat diet leads to an increase in the hepatic steatosis degree and the development of endoplasmic reticulum stress (31). Impaired bile acid metabolism in adult NAFLD patients is accompanied by a significant increased risk of liver damage (32). In addition, patients with nonalcoholic steatohepatitis are characterized by a higher level of postprandial bile acid release and a higher likelihood of liver damage by secondary bile acids (33). In our study, patients with TT-genotype of SNP rs11110390 *NR1H4* gene had significantly higher liver stiffness and demonstrated a tendency to increase the steatosis degree in the absence of significant lipid abnormalities, which contradicts the data of Heni et al. (2013) who confirmed the association of SNP rs11110390 *NR1H4* gene with fasting free fatty acids levels (21).

One of the reasons of liver stiffness changes in case of impaired FXR-signaling may be the activation of pro-inflammatory cascades due to increased intestinal permeability. An experimental study of Inagaki et al. (2006) demonstrated that FXR plays a crucial role in maintaining

the integrity of the intestinal epithelial barrier and preventing the development of bacterial overgrowth and bacterial translocation (34). In FXR-knockout mice an increase in intestinal paracellular permeability was observed due to a decrease in the expression of occludin. Furthermore, an increase in aerobic and anaerobic microflora presentation in the ileal mucosa and mesenteric lymph nodes was noticed. Moreover, FXR is able to directly selectively inhibit the NF-kB-associated inflammatory pathway and ensure hepatocyte survival (8). According to our data, changes in the liver stiffness in patients with CT- and TT-genotypes were accompanied by an increase in the concentration of IL-6 and TNF-α, but in heterozygous SNP carriers cytokine balance was maintained due to increased IL-10 production whereas in children with TT-genotype a significant reduction in the IL-10 level was observed, which led to a shift in the balance of pro- and anti-inflammatory cytokines toward inflammation.

Thus, our study demonstrated that the variability of the *NR1H4* gene (SNP rs11110390) is associated with an increased likelihood of developing NAFLD in children. Changes in the bile acid fractions distribution in patients with TT-genotype are characterized by a significant increase in TC and TDC in the gallbladder's and hepatic bile, accompanied by a significant increase in GGT level, increased liver stiffness and steatosis degree. Cytokine profile in children with CT-genotype of SNP rs11110390 *NR1H4* gene is characterized by higher levels of pro-inflammatory cytokines – IL-6, TNF-α, but maintaining the balance due to compensatory increase of IL-10, while children with TT-genotype are characterized by shift the balance towards pro-inflammatory cytokines due to reducing the IL-10 level. Taking into account the prevalence of TT-genotype of SNP rs11110390 *NR1H4* gene in the pediatric population (10.5%), features of the course of NAFLD in SNP carriers, obese NAFLD children with TT-genotype should be considered at risk of the disease progression, which requires timely correction.

CONCLUSION

TT-genotype of SNP rs11110390 *NR1H4* gene carriage are associated with an increased likelihood of NAFLD development in obese children. In children with TT-genotype of SNP rs11110390 *NR1H4* gene an increase in the liver stiffness and steatosis degree is observed in combination with an increase in taurine-conjugated fractions of bile acids in hepatic and gallbladder's bile connected with biochemical signs of cholestasis. In TT-genotype carriers of SNP rs11110390 *NR1H4* gene a shift of cytokine balance towards inflammation is observed due to reduction of IL-10 levels.

FUNDING

The study was conducted within the state budget research "To study the leading factors influencing the course of non-alcoholic liver steatosis in children, to develop prediction criteria of progression and to create a differentiated treatment algorithm", state registration number 0114U005583.

CONFLICTS OF INTEREST

Authors have no conflict of interest to declare.

REFERENCES

1. Stepanov YM, Abaturov OE, Zavhorodnia NY, Skirda IY. Non-alcoholic fatty liver disease in children: current view on diagnostics and treatment (Part I). Gastroenterologia 2015; 2: 99–107.
2. Mantovani A, Zusi C. The dawn of a new era for nonalcoholic fatty liver disease? Hepatobiliary Surg Nutr 2019; 8(Suppl 6): 629–31.
3. van der Sijde MR, Ng A, Fu J. Systems genetics: From GWAS to disease pathways. Biochim Biophys Acta 2014; 1842(Suppl 10): 1903–9.
4. Goldner D, Lavine JE. Nonalcoholic Fatty Liver Disease in Children: Unique Considerations and Challenges. Gastroenterology 2020; 158(Suppl 7): 1967–83.
5. Ismaiel A, Dumitrascu DL. Genetic predisposition in metabolic-dysfunction-associated fatty liver disease and cardiovascular outcomes-Systematic review. Eur J Clin Invest 2020; 50: e13331.
6. Zusi C, Mantovani A, Olivieri F, et al. Contribution of a genetic risk score to clinical prediction of hepatic steatosis in obese children and adolescents. Dig Liver Dis 2019; 51: 1586–92.
7. Sookoian S, Pirola CJ, Valenti L, Davidson NO. Genetic Pathways in Nonalcoholic Fatty Liver Disease: Insights From Systems Biology. Hepatology 2020; 72(Suppl 1): 330–46.
8. Chen, X, Wang L, Shan Q, et al. A novel heterozygous NR1H4 termination codon mutation in idiopathic infantile cholestasis. World J Pediatr 2012; 8(Suppl 1): 67–71.
9. Gomez-Ospina N, Potter C, Xiao R, et al. Mutations in the nuclear bile acid receptor FXR cause progressive familial intrahepatic cholestasis. Nat Commun 2016; 7: 10713.
10. Pavlovic N, Stanimirov B, Mikov M. Bile Acids as Novel Pharmacological Agents: The Interplay Between Gene Polymorphisms, Epigenetic Factors and Drug Response. Curr Pharm Des 2017; 23(Suppl 1): 187–215.
11. Ticho AL, Malhotra P, Dudeja PK, Gill RK, Alrefai WA. Intestinal Absorption of Bile Acids in Health and Disease. Compr Physiol 2019; 10(Suppl 1): 21–56.
12. Koutsounas I, Theocharis S, Delladetsima I, Patsouris E, Giaginis C. Farnesoid X receptor in human metabolism and disease: the interplay between gene polymorphisms, clinical phenotypes and disease susceptibility. Expert Opin Drug Metab Toxicol 2015; 11(Suppl 4): 523–32.
13. Hiebl V, Ladurner A, Latkolik S, Dirsch VM. Natural products as modulators of the nuclear receptors and metabolic sensors LXR, FXR and RXR. Biotechnol Adv 2018; 36(Suppl 6): 1657–98.
14. Veselsky SP, Lyashchenko PS, Lukyanenko IA. Method for determination of bile acids in biological fluids. Laboratory Work 1979; 3: 176–81.
15. National Center for Biotechnology Information U.S. National Library of Medicine. ALFA: Allele Frequency Aggregator. (Accessed March 10, 2020, at www.ncbi.nlm.nih.gov/snp/docs/gsr/alfa/.)
16. Nijmeijer RM, Gadaleta RM, van Mil SW, et al. Farnesoid X receptor (FXR) activation and FXR genetic variation in inflammatory bowel disease. PLoS One 2011; 6(Suppl 8): e23745.
17. Lutz P, Berger C, Langhans B, et al. A farnesoid X receptor polymorphism predisposes to spontaneous bacterial peritonitis. Dig Liver Dis 2014; 46: 1047–50.
18. van den Berg SW, Dollé ME, Imholz S, et al. Genetic variations in regulatory pathways of fatty acid and glucose metabolism are associated with obesity phenotypes: a population-based cohort study. Int J Obes (Lond) 2009; 33: 1143–52.
19. Hu M, Lui SS, Tam LS, Li EK, Tomlinson B. The farnesoid X receptor -1G>T polymorphism influences the lipid response to rosuvastatin. J Lipid Res 2012; 53: 1384–9.
20. Liu M, Wu XJ, Zhao GL, et al. Effects of Polymorphisms in NR1H4, NR1I2, SLCO1B1, and ABCG2 on the Pharmacokinetics of Rosuvastatin in Healthy Chinese Volunteers. J Cardiovasc Pharmacol 2016; 68: 383–90.
21. Heni M, Wagner R, Ketterer C, et al. Genetic variation in NR1H4 encoding the bile acid receptor FXR determines fasting glucose and free fatty acid levels in humans. J Clin Endocrinol Metab 2013; 98: E1224–9.
22. Attinkara R, Mwinyi J, Truninger K, et al. Association of genetic variation in the NR1H4 gene, encoding the nuclear bile acid receptor FXR, with inflammatory bowel disease. BMC Res Notes 2012; 5: 461.
23. Kovacs P, Kress R, Rocha J, et al. Variation of the gene encoding the nuclear bile salt receptor FXR and gallstone susceptibility in mice and humans. J Hepatol 2008; 48: 116–24.

24. Alashkar F, Weber SN, Vance C, et al. Persisting hyperbilirubinemia in patients with paroxysmal nocturnal hemoglobinuria (PNH) chronically treated with eculizumab: The role of hepatocanalicular transporter variants. Eur J Haematol 2017; 99: 350–6.
25. Dixon PH, Wadsworth CA, Chambers J, et al. A comprehensive analysis of common genetic variation around six candidate loci for intrahepatic cholestasis of pregnancy. Am J Gastroenterol 2014; 109(Suppl 1): 76–84.
26. Van Mil SW, Milona A, Dixon PH, et al. Functional variants of the central bile acid sensor FXR identified in intrahepatic cholestasis of pregnancy. Gastroenterology 2007; 133(Suppl 2): 507–16.
27. Patrushev LI, Kovalenko F. Functions of non-coding sequences of the mammalian genome. Adv Biol Chem 2014; 54: 39–102.
28. Ramírez-Bello J, Jiménez-Morales M. Functional implications of single nucleotide polymorphisms (SNPs) in protein-coding and non-coding RNA genes in multifactorial diseases. Gac Med Mex 2017; 153(Suppl 2): 238–50.
29. Chiang JYL, Ferrell JM. Bile acid receptors FXR and TGR5 signaling in fatty liver diseases and therapy. Am J Physiol Gastrointest Liver Physiol 2020; 318(Suppl 3): G554–G573.
30. Sinal CJ, Tohkin M, Miyata M, Ward JM, Lambert G, Gonzalez FJ. Targeted disruption of the nuclear receptor FXR/BAR impairs bile acid and lipid homeostasis. Cell 2000; 102(Suppl 6): 731–44.
31. Alvarez-Sola G, Uriarte I, Latasa MU, et al. Fibroblast growth factor 15/19 (FGF15/19) protects from diet-induced hepatic steatosis: development of an FGF19-based chimeric molecule to promote fatty liver regeneration. Gut 2017; 66: 1818–28.
32. Mouzaki M, Wang AY, Bandsma R, et al. Bile Acids and Dysbiosis in Non-Alcoholic Fatty Liver Disease. PLoS One 2016; 11(Suppl 5): e0151829.
33. Ferslew BC, Xie G, Johnston CK, et al. Altered Bile Acid Metabolome in Patients with Nonalcoholic Steatohepatitis. Dig Dis Sci 2015; 60(Suppl 11): 3318–28.
34. Inagaki T, Moschetta A, Lee YK, et al. Regulation of antibacterial defense in the small intestine by the nuclear bile acid receptor. Proc Natl Acad Sci U S A 2006; 103(Suppl 10): 3920–5.

A Missed Diagnosis of Laryngotracheal Injury Secondary to Emergency Intubation: Lessons Learned

V Sha Kri Eh Dam[1,2,*], Sakinah Mohamad[2], Nik Fariza Husna Nik Hassan[3], Mohd Zulfakar Mazlan[4]

ABSTRACT

Iatrogenic laryngotracheal trauma is a potentially fatal complication of endotracheal intubation, especially in an emergency setting. Symptoms are almost always related to speech, breathing, and swallowing. Hoarseness being the commonest symptom, while shortness of breath and stridor always signify more devastating injury. We present a case of iatrogenic subglottic and tracheal stenosis, which was misdiagnosed in the emergency department during the first visit. This case report highlights the importance of salient history and thorough examination with a high index of suspicion in a stridorous case with a recent history of intubation. Early detection and management are vital to avoid a life-threatening event.

KEYWORDS

endotracheal intubation; laryngotracheal trauma; tracheostomy

AUTHOR AFFILIATIONS

[1] Department of Otorhinolaryngology-Head & Neck Surgery, Hospital Tengku Ampuan Rahimah, Jalan Langat, 41200 Klang, Selangor, Malaysia
[2] Department of Otorhinolaryngology-Head and Neck Surgery, School of Medical Sciences, Universiti Sains Malaysia Health Campus, 16150 Kota Bharu, Kelantan, Malaysia
[3] Speech Pathology Programme, School of Health Sciences, Universiti Sains Malaysia Health Campus, 16150 Kota Bharu, Kelantan, Malaysia
[4] Department of Anaesthesiology and Intensive Care, School of Medical Sciences, Universiti Sains Malaysia Health Campus, 16150 Kota Bharu, Kelantan, Malaysia
* Corresponding author: Department of Otorhinolaryngology-Head & Neck Surgery, Hospital Tengku Ampuan Rahimah, Jalan Langat, 41200 Klang, Selangor, Malaysia; e-mail: kridamrong@gmail.com

Received: 6 September 2021
Accepted: 30 October 2022
Published online: 2 February 2023

Acta Medica (Hradec Králové) 2022; 65(3): 112–117
https://doi.org/10.14712/18059694.2022.27

INTRODUCTION

Larynx and trachea are vital organs providing important functions for breathing, phonation, and swallowing. The laryngotracheal complex consists of a cartilaginous framework supported by a variety of muscular and ligamentous soft tissue structures (1). Injury to these structures should alert physicians of the potential airway compromise and challenges in the management.

The mechanism of laryngotracheal injury can be classified into external and internal. The former is further classified into blunt and penetrating injuries, while the latter always due iatrogenic and inhalation injuries (2). Intubation probably being the leading cause of iatrogenic injury now due to its widespread use to secure the airway. Larynx being the most common site of the injury secondary to endotracheal intubation, while trachea and oesophageal injuries are more frequently associated with difficult intubation (2).

Endotracheal intubation (ETI) remains the goal standard procedure for airway management (3). However, it can cause complications, some of which are life-threatening, like laryngeal trauma, subglottic stenosis, and tracheal rupture. It is well accepted that post-intubation laryngotracheal injury is related to the duration of intubation. Injury following short term intubation in an elective setting is rare, accounting about 6.3% (4). The percentage was likely to be higher in the emergency setting due to inadequate evaluation of the airway or preparation of the patient and equipment.

Other risk factors for the injury are excessive cuff pressure, inappropriate endotracheal tube (ETT) size, difficult airway patient, use of introducers like stylet or bougie, inadequate muscle relaxant, and inexperience of person performing intubation (3, 5). Besides that, patient-specific factors such as female sex, cigarette smoking, and gastroesophageal reflux disease also have been shown to play a role (6).

Symptoms of intubation related laryngotracheal injury are almost always related to speech, breathing, and swallowing. The patient may present with dysphonia, aphonia, hoarseness, shortness of breath, stridor, sore throat, dysphagia, and odynophagia. Most of the symptoms are usually resolved by 48 hours. Thus, more devasting injury should be suspected if symptoms last more than 72 hours (7).

The most common lesion is vocal cord hematoma, followed by mucosal thickening with oedema, mucosal laceration, laceration of vocalis muscle, arytenoid subluxation, and contact ulcer with or without granuloma formation and vocal cord immobility (6). Vocal cord immobility is the result of either cricoarytenoid joint dislocation, inter-arytenoid scar or recurrent laryngeal nerve palsy. There are reported case of tracheal rupture, however, it is rare (8).

The long-term management is depending on the type of injury and severity, whilst in the short term, patients may benefit from a tracheostomy in severe cases. Here, we report a case of missed diagnosis of subglottic and tracheal stenosis secondary to emergency intubation, how we managed the patient and lessons learnt.

CASE REPORT

A 16-year-old boy presented with progressive worsening of shortness of breath for three days duration. He had a history of intubation after alleged motor vehicle accident six days before the current presentation. At that time, he was brought to the hospital by ambulance with Glasgow Coma Score (GCS) of 7/15 and was intubated at the Emergency Department (ED) with a cuffed ETT size 7.5 mm (inner diameter), anchored at 21 cm for airway protection. However, there was no documentation of any difficulty of intubation as well as the number of attempts of intubation. He was admitted to the Intensive Care Unit (ICU) overnight, extubated on the following day, and transferred to the general surgical ward. Apart from the severe traumatic brain injury (without intracranial bleed), he also sustained a closed fracture of the left distal radius. He was discharged home on day 4 of admission.

The shortness of breath was actually noticed at home after being discharged. It was initially tolerable then progressively worsening until he was unable to lie flat and needed to sleep in a sitting position. It was associated with hoarseness, weak voice, odynophagia, noisy breathing and non-productive cough. He visited ED one day after been discharged due to worsening shortness of breath. He was treated as atypical pneumonia and discharged home with antibiotics. Unfortunately, he presented again to ED in less than 24 hours as his symptoms became more severe.

On examination, he was lethargic-looking with the presence of inspiratory stridor, hoarseness, tachypneic with a respiratory rate of 22 breaths/min and subcostal recessions. Besides that, his maximum phonation time was 7 seconds, unable to count one to ten in a single breath but with a good cough quality suggestive of inadequate subglottic pressure but with good glottic closure. His oxygen saturation (SpO_2) and arterial blood gas (ABG) were still within the normal range. However, sequential ABG showed a rising pattern of carbon dioxide (CO_2) level. A referral to Otorhinolaryngology (ORL) team was done and flexible nasopharyngolaryngoscopy (FNPLS) performed at ED revealed some granulation tissues at the subglottic region with a small airway opening seen at the posterior part of the subglottic region. Supraglottic and glottic structures were normal-looking and bilateral vocal cords were mobile symmetrically.

Lateral soft tissue neck X-ray demonstrated soft tissue thickening with narrowing of the airway from C5 to C7 cervical vertebra (Figure 1). Otherwise, chest X-ray showed a relatively clear lung field. Since he was stable, computerized tomography (CT) scan of the neck was done for more details regarding the anatomical obstruction. The CT scan revealed circumferential subglottic soft tissue thickening extending from the level of the lower border of C5 to lower border of C7 cervical vertebrae, causing subglottic and tracheal stenosis (Figure 2). The length of the stenosis was 3 cm, with the narrowest segment width of 4 mm. Lower trachea and bilateral primary bronchi were preserved.

The patient was then subjected to emergency tracheostomy, direct laryngoscopy, and tracheoscopy to secure and then assess the airway. The patient was intubated with

Fig. 1 Lateral soft tissue neck X-ray shows soft tissue thickening with narrowing of airway from level of C5 to C7 cervical vertebra.

Fig. 2 Sagittal view, soft tissue window of contrasted CT scan of neck shows circumferential soft tissue thickening extending from level of lower border of C5 to lower border of C7 cervical vertebra causing subglottic and tracheal stenosis.

cuffed micro-laryngeal tube (MLT) size 4.0 mm (inner diameter), anchored at 22 cm on the third attempt after failed two attempts with larger ETT. Tracheostomy was performed under general anaesthesia and was uneventful. A cuffed tracheostomy tube size 7.5 mm (inner diameter) was inserted between the 3rd and 4th tracheal rings. Through the upper part of the tracheal incision, the stenotic segment was seen just above the 3rd tracheal ring. Direct laryngoscopy showed pinkish-red granulation tissue in the subglottic region. Tracheoscopy revealed the total length of the stenotic segment was about 38 mm, starting from 5 mm below the true vocal cord to 4 mm above tracheostoma. There was presence of immature granulation tissue at the anterior part of the tracheal wall and mucosal tear at the left posterolateral part of the tracheal wall causing false tract (Figure 3). In addition, there was some slough at the posterior commissure. Luminal obstruction by the stenotic segment was measured by about 78% thus, it was Cotton-Myer grade III. He was started on intrave-

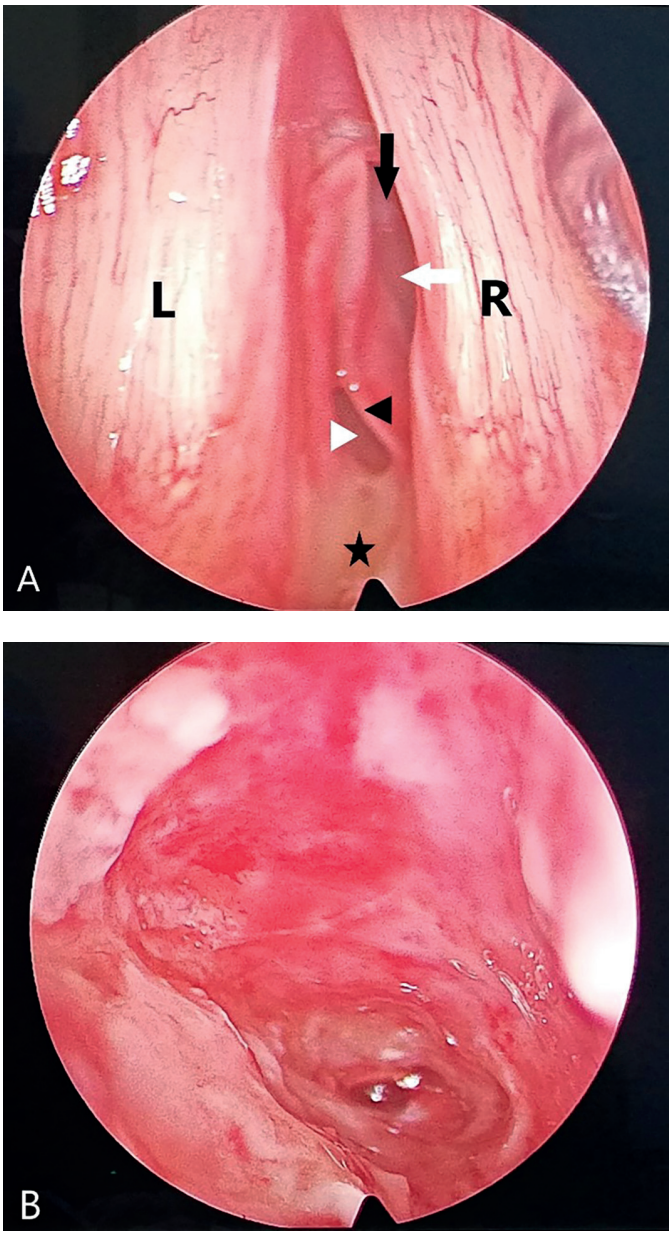

Fig. 3 A. Endoscopic view of the subglottic region shows present of granulation tissue at the anterior part (black arrow) with narrowed subglottic region (white arrow), mucosal tear at the left posterolateral part (black arrow head) causing false tract (white arrow head) and present of slough at the posterior part (star). L: left vocal cord; R: Right vocal cord. B. Endoscopic view of trachea shows narrowed tracheal lumen with present of granulation tissues and slough.

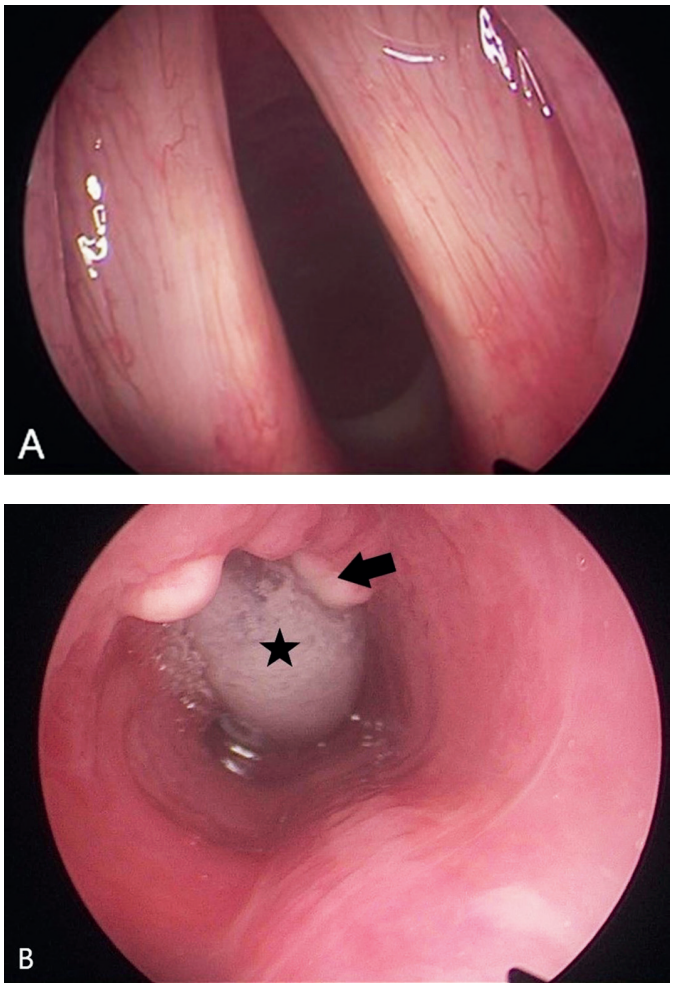

Fig. 4 Endoscopic view of the subglottic (A) and trachea (B) after 2 weeks shows well healed subglottic and tracheal wall with minimal granulation tissue (arrow) at the superior part of tracheostoma and tracheostomy tube (star).

nous (IV) dexamethasone 8 mg three times daily (TDS) for three days to reduce the tissue oedema and inflammation, and IV Augmentin, 1.2 g TDS for five days to cover for infection.

The patient was discharged home after five days of observation in the ward, and the tracheostomy tube was changed to uncuffed tube sized 7.5 mm (inner diameter). He was well and underwent another direct laryngoscopy and tracheoscopy under general anaesthesia about two weeks later. Unexpectedly, it revealed a well-healed subglottic and tracheal wall with just minimal granulation tissue at the superior part of tracheostoma (Figure 4). The tracheostomy tube was then changed to a smaller size, spigotted and subsequently decannulated successfully. He was well and remained asymptomatic even after six months follow-up.

DISCUSSION

Intubation related laryngotracheal injury is common, as high as 73% in patients intubated for more than 24 hours, and larynx is more common than trachea to be injured (5, 9). Short term intubation less than 24 hours and in the elective setting is relatively rare causing laryngotracheal injury (4). The injuries are ranging from mild to severe and life-threatening conditions.

In our case, the patient was able to be extubated in less than 24 hours after intubation. However, the laryngotracheal injury was so extensive which required tracheostomy to secure the airway. By Bernoulli's principle, when a patient is breathing rapidly, the air flows through a severely narrowed airway (in this case, through the stenosed subglottic and upper tracheal regions) causes that restricted area to collapse and later on becomes more oedematous. Therefore, tracheostomy helps to rest that area to heal and to prevent more complications apart from securing the airway. In this case, the tracheostomy was inserted slightly lower than usual (between 2nd and 3rd tracheal rings), distal to the site of stenosis to avoid the area of laryngotracheal injury. We also noticed the presence of immature granulation tissue and mucosal tear with a false track (as shown in Figure 3), which could be the results of traumatic injury during intubation. This injury may happen in an emergency setting where everything needs to be acted fast, especially when dealing with the airway. Study also showed laryngeal injury is more common in emergency intubation (5). Besides that, if a restless patient with GCS 7/15 was not properly relaxed during intubation, this can increase the risk of laryngotracheal injury.

Post-extubation patients may experience a variety of symptoms. Hoarseness is the commonest symptom followed by sore throat and odynophagia (4, 9). A systemic review revealed that hoarseness and vocal cords injury are relatively common following short-term general anaesthesia (10). In the vast majority, this symptom is temporary and lasts on a mean two to three days (11). However, in a case of persistent symptoms with dyspnoea and stridor, a more serious complication should be suspected. Our patient presented with worsening obstructive symptoms and hoarseness for more than three days; however, he was discharged home and treated as pneumonia on the first visit to ED. Although pneumonia is also a common condition in patients of post-intubation and ICU admission, intubation related laryngotracheal injury should always be suspected in this type of patient and presentation.

Pneumonia may share some similar symptoms with intubation related laryngotracheal injury. Thus, further investigation should be carried out. This is including a simple neck and chest X-ray. Only a chest X-ray was performed during the first visit; thus, the diagnosis of laryngotracheal injury was missed. A simple clinical examination such as FNPLS can be performed in the ED setting by a skilled operator, which provides excellent visualization of the supraglottic, glottic, and possible subglottic region. In our case, granulation tissue was seen in the subglottic region, causing narrowing of the airway, otherwise normal supraglottic and glottic structures, and mobility of vocal cords. However, it is to note that, in certain cases such as suspected acute epiglottitis in children, the contact of the tip of the scope with the epiglottis or laryngeal mucosa may cause laryngospasm and upper airway "shut-down".

Besides laryngotracheal stenosis, differential diagnosis of stridor with history of intubation would include edema of the vocal cord or subglottic region, vocal cord granuloma, vocal cord palsy, cricoarytenoid dislocation, webbing

of anterior commissure and tracheomalacia especially in prolonged intubation. Stridor is one of the red flag signs for airway emergency. Stridor is different from stertor. Stridor is defined as high-pitched sound, caused by partial obstruction of the airway due to abnormal apposition of two tissue surfaces in proximity, with resultant in turbulent airflow (12). In contrast, stertor is a low-pitched, mainly inspiratory sound that may be produced by obstructing lesions of the nasopharynx, oropharynx and hypopharynx (13). The quality of the stridor may give clue to site of obstruction as seen in table 1 (12).

Tab. 1 Different quality of stridor pointing towards different sites of obstruction.

Quality of stridor	Site(s) of obstruction
Inspiratory	Supraglottic region (epiglottis, aryepiglottic folds and false cords) Glottic region
Expiratory	Trachea region and below
Biphasic (combination of inspiratory and expiratory stridor)	Glottic Subglottic region

CT scan of the neck is usually not required before tracheostomy, as securing the airway is more urgent. However, since the patient was stable and a long segment of airway narrowing was seen in lateral neck X-ray, the CT scan neck was performed. CT scan provides a better anatomical description of the injury and helps in surgical planning. CT scan gives details of the approximate length of stenotic segment, narrowest diameter of tracheal lumen, distance of upper end of stenotic segment with the true cords, whether it is single or multisegmented stenosis and level of lower end of stenotic segment. It is important in preventing performing tracheostomy through the injury site, which may result in intractable bleeding.

Not all of our patients are as fortunate as in this case whereby a near-complete resolution is achieved within 2 weeks with conservative management post-tracheostomy. The patient was subsequently treated with IV dexamethasone for three days and IV antibiotics for five days post-tracheostomy. This may suggest that if the problem is actually detected earlier post-extubation and treated conservatively with steroids and antibiotics, the patient may not require tracheostomy but this is not true for all patients. Systemic corticosteroid, antibiotic, and closed observation probably would be sufficient (14). The potential benefit of steroids is still open to debate and presumably based on its anti-inflammatory actions (15). The antibiotic was started in our case in view of the presence of the slough at the posterior commissure which suggest infection. Some studies suggested that additional anti-inflammatory property that presence in certain antibiotic may has a beneficial effect on laryngotracheal stenosis (16, 17). In contrast, if the diagnosis is further delayed, the patient may lose his airway. This situation is very challenging in management, which the patient may present with cardiorespiratory distress, and tracheostomy may need to be performed under local anaesthesia at the ED itself. This undoubtedly results in higher mortality and morbidity.

This complication of laryngotracheal stenosis is preventable. First of all, recognition of patients with risk of difficult airway is very crucial. About 10% of patients were found to be difficult for intubation (18). Physician can anticipate difficult intubation in patients with class 3 on upper lip bite test, shorter hyo-mental distance of <3.0–5.5 cm, retrognathia, obese and modified Mallampati score ≥ 3 (18). The mentioned risk factors were not found in our case. Senior physician and/or anaesthetic team should be alerted immediately when facing difficult intubation. Careful intubation taking into accounts of the appropriate ETT size, using low pressure cuffs and avoiding unnecessary trauma, especially in emergency settings, is fundamental in preventing laryngotracheal injury. Other strategies for intubation of difficult airways include awake intubation, video-assisted laryngoscopy, fiberoptic-guided intubation, using stylets (with/without light) or tube changers, and supraglottic airway ventilation for example laryngeal mask airway (LMA) (19). Judicious care should be carried out through the whole intubation period. It is recommended to use soft pressure–high volume ETT and regular checking of cuff pressure to maintain the cuff pressure around 25 cm H_2O (5). Apart from that, managing team should optimize patient and try aiming for early extubation as prolonged intubation is one of the risk factors for laryngotracheal stenosis.

CONCLUSION

Intubation related laryngotracheal injuries are ranging from mild to potential life-threatening. Stridorous patient with history of emergency intubation although duration is short should always give a high index of suspicion for subglottic and tracheal stenosis. Junior doctors should be able to recognize and detect this clinical entity early, and manage accordingly. Despite extensive subglottic/tracheal stenosis, this case was still manageable with a tracheostomy followed by conservative treatments.

LEARNING POINTS

- Physician should have a high index of suspicion for subglottic and/or tracheal stenosis in a case of stridorous patient with a history of emergency intubation.
- Simple imaging such as neck X-ray together with chest X-ray helps in establishing the diagnosis of subglottic/tracheal stenosis as well as ruling out other pathologies.
- Junior doctors should be able to recognize patients with difficult intubation, alert their seniors and urgently refer to anesthetic team when facing a difficult intubation.
- The severity of injury during intubation is a more significant factor than the duration of intubation in this case.
- Some cases of subglottic/tracheal stenosis may be successfully managed with a tracheostomy followed by conservative treatments with systemic corticosteroid and antibiotic, based on their anti-inflammatory property (15–17).

REFERENCES

1. Burdett E, Mitchell V. Anatomy of the larynx, trachea and bronchi. Anaesth Int Care Med 2008; 9: 329–33.
2. Domino KB, Posner KL, Caplan RA, Cheney FW. Airway injury during anesthesia: A closed claims analysis. Anesthesiology 1999; 91(6): 1703–11.
3. Divatia JV, Bhowmick K, Kaushik. Complications of endotracheal intubation and other airway management procedures. Indian J Anaesth 2005; 49: 308–18.
4. Peppard SB, Dickens JH. Laryngeal injury following short-term intubation. Ann Otol Rhinol Laryngol 1983; 92: 327–30.
5. Tadié JM, Behm E, Lecuyer L, et al. Post-intubation laryngeal injuries and extubation failure: a fiberoptic endoscopic study. Intensive Care Med 2010; 36: 991–8.
6. Evans D, McGlashan J, Norris A. Iatrogenic airway injury. BJA Education 2015; 15(4): 184–9.
7. Mota LA, de Cavalho GB, Brito VA. Laryngeal complications by orotracheal intubation: Literature review. Int Arch Otorhinolaryngol 2012; 16(2): 236–45.
8. Ovari A, Just T, Dommerich S, Hingst V, Bottcher A, Schuldt T, et al. Conservative management of post-intubation tracheal tears-report of three cases. J Thorac Dis 2014; 6(6): E85–91.
9. Kastanos N, Estopá Miró R, Marín Perez A, Xaubet Mir A, Agustí-Vidal A. Laryngotracheal injury due to endotracheal intubation: Incidence, evolution, and predisposing factors. A prospective long-term study. Crit Care Med 1983; 11: 362–7.
10. Martins RH, Braz JR, Dias NH, Castilho EC, Braz LG, Navarro LH. Hoarseness after tracheal intubation. Revista brasileira de anestesiologia 2006; 56(2): 189–99.
11. Mendels EJ, Brunings JW, Hamaekers AE, Stokroos RJ, Kremer B, Baijens LW. Adverse laryngeal effects following short-term general anesthesia: A systematic review. Arch Otolaryngol Head Neck Surg 2012; 138: 257–64.
12. Ida JB, Thompson DM. Pediatric stridor. Otolaryngol Clin North Am 2014; 47(5): 795–819.
13. Leon-Astudillo C, Lee GS, Katwa U. An unusual case of noisy breathing in an infant. J Clin Sleep Med 2019; 15(1): 149–52.
14. Loh K, Irish J. Complications of endotracheal intubation and other airway management procedures. Anesth Clin North Am 2002; 20: 953–69.
15. Lee CH, Peng MJ, Wu CL. Dexamethasone to prevent postextubation airway obstruction in adults: A prospective, randomized, double-blind, placebo-controlled study. Crit Care 2007; 11(4): R72.
16. Huang Z, Wei P, Gan L, et al. Protective effects of different anti-inflammatory drugs on tracheal stenosis following injury and potential mechanisms. Mol Med Rep 2021; 23(5): 314.
17. Sanders JG, Jean-Louis MF. A case of subglottic and diffuse tracheal stenoses appearing responsive to macrolide therapy. N Z Med J 2012; 125(1366): 68–73.
18. Detsky ME, Jivraj N, Adhikari NK, et al. Will this patient be difficult to intubate?: The rational clinical examination systematic review. JAMA 2019; 321(5): 493–503.
19. Apfelbaum JL, Hagberg CA, Caplan RA, et al. Practice guidelines for management of the difficult airway: an updated report by the American Society of Anesthesiologists Task Force on Management of the Difficult Airway. Anesthesiology 2013; 118(2): 251–70.